

Comparison of *in vitro* and *in situ* plankton production determinations

Carol Robinson^{1,3,*}, Gavin H. Tilstone¹, Andrew P. Rees¹, Timothy J. Smyth¹, James R. Fishwick¹, Glen A. Tarran¹, Boaz Luz², Eugeni Barkan², Efrat David²

¹Plymouth Marine Laboratory, Prospect Place, West Hoe, Plymouth PL1 3DH, UK

²The Institute of Earth Sciences, Hebrew University, Jerusalem 91904, Israel

³Present address: University of East Anglia, School of Environmental Sciences, Norwich NR4 7TJ, UK

ABSTRACT: Plankton production was measured using 8 techniques at 4 stations in the Celtic Sea, North Atlantic Ocean, in April 2002. Primary production (PP) was derived from ¹⁴C incorporation into particulate carbon after 24 h simulated *in situ*, PP(¹⁴C_{SIS}), and 2 h photosynthesis-irradiance incubations, PP(¹⁴C_{PUR}), and from 2 published satellite algorithms, PP_(VGPM) and PP_(M91). Gross production (GP) was calculated from O₂ evolution, GP(O₂), and ¹⁸O enrichment of dissolved O₂, GP(¹⁸O), after 24 h simulated *in situ* incubations, and from *in situ* active fluorescence measured by fast repetition rate fluorometry (FRRF). Net community production (NCP) was determined from changes in *in situ* dissolved oxygen, NCP(ΔO₂), and from changes in oxygen during 24 h simulated *in situ* incubations, NCP(O₂). Dark community respiration (DCR) was derived from changes in oxygen during a 24 h dark incubation, DCR(O₂), and daily oxygen uptake, DOU(¹⁸O, O₂), was calculated from the difference between GP(¹⁸O) and NCP(O₂). Three stations were dominated by picoautotrophs and the fourth station was dominated by diatoms. While most of the comparisons between techniques fell within previously published ranges, 2 anomalies occurred only at the diatom-dominated station. Rates of PP(¹⁴C_{PUR}) were < rates of PP(¹⁴C_{SIS}), and oxygen uptake in the light was more than 10-fold > oxygen uptake in the dark. The low rates of PP(¹⁴C_{PUR}) in relation to PP(¹⁴C_{SIS}) may have resulted from the heterogeneous nature of the bloom and differences in sampling time. However, it is also possible that dissolved organic material (DOM) released by the stressed diatom population restricted the diffusion of ¹⁴C into the cells, thereby causing a greater underestimate of PP by techniques using short incubations. The significantly higher rates of oxygen uptake in the light are difficult to reconcile, and we do not know whether the light enhanced oxygen uptake was directly linked to carbon fixation. However, the release of DOM may also have provided substrate for enhanced respiration in the light. These anomalies were only revealed through the concurrent measurement of plankton production by this wide range of techniques. Further investigation of DOM excretion and light-enhanced respiration during diatom blooms is warranted.

KEY WORDS: Plankton production · Respiration · Oxygen · Fast repetition rate fluorometry · Satellite algorithms

Resale or republication not permitted without written consent of the publisher

INTRODUCTION

The magnitude of plankton primary production is among the most crucial determinations made by biological oceanographers. Unfortunately, none of the currently available methods of determining primary production provides a definitive measurement. The

H¹⁴CO₃⁻ assimilation method is the most commonly used, and is also the most persistently criticised (Longhurst et al. 1995). The dissolved oxygen or dissolved inorganic carbon (DIC) concentration light/dark bottle incubation assumes that respiration occurs at the same rate in the dark as in daylight, and the mass spectrometric determination of ¹⁸O-labelled O₂ produced

*Email: carol.robinson@uea.ac.uk

from ^{18}O -labelled H_2O measures all oxygen-producing metabolic processes, even those not related to organic carbon assimilation (Bender et al. 1999). Primary production estimates derived from any of these methods also need to be interpreted in view of the measurement time and space scales used and any potential methodological artefacts due to containment and incubation conditions. Until an unambiguous technique is developed and a suitably large database is accumulated, comparisons between estimates derived from different methods can constrain the range of uncertainty and inform our understanding of the physiological and ecological processes involved. However, surprisingly few direct comparisons of 2 or more methods have been made.

Since the ^{14}C technique measures a rate approximating net production (Karl et al. 2002, Marra 2002), ^{14}C incorporation is less than gross production derived from changes in dissolved O_2 [$\text{GP}(\text{O}_2)$] by a factor of 0.4 to 0.8 (Aristegui et al. 1996, Robinson et al. 1999, 2002, Rees et al. 2002). Comparisons between the ^{14}C and ^{18}O methods yield ^{14}C uptake:gross ^{18}O production [$\text{GP}(^{18}\text{O})$] ratios between 0.4 and 1.0, with recent open ocean studies converging on ratios of 0.4 to 0.5 (Bender et al. 1987, 1999, Laws et al. 2000, Dickson et al. 2001). O_2 concentration and ^{18}O -derived estimates of marine gross production yield $\text{GP}(\text{O}_2):\text{GP}(^{18}\text{O})$ ratios between 0.3 and 1.0 (Grande et al. 1989a, Dickson & Orchardo 2001), while $\text{GP}(\text{O}_2):\text{GP}(^{18}\text{O})$ ratios up to 3.5 have been measured in nutrient rich, low oxygen estuarine systems (Gazeau et al. 2007). Only 3 marine studies have compared production rates derived from more than 2 *in vitro* methods (Bender et al. 1987, Grande et al. 1989a, Kiddon et al. 1995), while several have compared rates derived from *in vitro* bottle incubations, e.g. of net community production (NCP = gross production minus autotrophic and heterotrophic respiration), ^{14}C or ^{15}N uptake with *in situ* changes in a photosynthetic product or substrate (Williams & Purdie 1991, Bender et al. 1992, 2000, Chipman et al. 1993, Dickson & Orchardo 2001, Rees et al. 2001, Marra 2002). The development of new methods for the determination of primary production inevitably requires comparison with more established (though not necessarily more accurate) techniques before they are widely adopted. Pump and probe, and fast repetition rate fluorometry (FRRF) allow phytoplankton production to be measured *in situ* at spatial (<1 m) and temporal (~1 s) resolutions that cannot be achieved with incubation experiments (Boyd et al. 1997, Moore et al. 2006). Concurrent estimates of integrated gross production derived from the FRRF were lower than those based on 24 h ^{14}C incubations in the Celtic Sea (Smyth et al. 2004) or comparable to those derived from 24 h oxygen light/dark bottle incubations in Sagami Bay, central

Japan (Sarma et al. 2005). An ideal representation of marine primary production is at the ocean basin and daily scale, and this can only be achieved from space. The global operation of ocean colour satellites and refinement to algorithms estimating primary production from ocean colour are beginning to enable comparison between estimates of primary production from space and estimates derived from *in situ* measurements and bottle incubations (Behrenfeld & Falkowski 1997, Joint & Groom 2000, Smyth et al. 2005, Tilstone et al. 2005). Comparisons between primary production estimates derived from different remote sensing (RS) models range over a factor of 2 (Carr et al. 2006), while comparisons between RS models and concomitant primary production measurements agree to within a factor of 0.35 to 2 (Campbell et al. 2002, Tilstone et al. 2005).

Remotely sensed images of ocean colour can also be used to guide shipboard sampling of phytoplankton blooms, revealing temporal and spatial heterogeneity and short term changes in the magnitude of phytoplankton pigment not previously realised (e.g. Holligan et al. 1993). The present study was undertaken in the northwest Celtic Sea in April 2002 and used a sampling approach informed by near real time (<1 d) images of ocean colour. This enabled us to sample high and low chlorophyll-containing waters and thereby facilitated a comparison of different methods of determining primary production. To our knowledge, this is the first time that primary production has been derived concurrently from 4 *in vitro* methods (^{14}C [24 h natural light and 2 h photosynthesis versus irradiance incubations], O_2 concentration and ^{18}O bottle incubations), 2 *in situ* techniques (ΔO_2 and FRRF) and 2 RS algorithms. We aimed to address the questions: How do these methods compare and contrast in their representation of a shelf edge spring diatom bloom? and Do these comparisons concur with comparisons made previously in other plankton communities?

MATERIALS AND METHODS

Sampling strategy. RRS 'Discovery' left Southampton, UK, on 1 April 2002 for a 14 d oceanographic study in the Celtic Sea southwest of Ireland between 48°N and 51°N , and 5°W and 12°W . Samples were collected on 2 April at a station (Stn 1, equivalent to Stn E1 in Southward et al. 2005) ca. 40 km southwest of Plymouth, Devon, UK, at $50^\circ 02'\text{N}$, $4^\circ 22'\text{W}$, on 3 April 2002 at a station (Stn 4) on the continental shelf at $49^\circ 32'\text{N}$, $6^\circ 00'\text{W}$ and on 5 April at a station (Stn 6) off the continental shelf at $48^\circ 41'\text{N}$, $11^\circ 12'\text{W}$. The major portion of the study focussed on the Great Sole Bank (Stn 7) at $49^\circ 37'\text{N}$, $10^\circ 20'\text{W}$, where a ring-shaped

buoy incorporating an ARGOS beacon and light, ballast chain and net drogue was deployed on 5 April 2002. Sampling was then undertaken alongside the buoy between 02:00 h and 16:00 h GMT each day for the following 7 d (Table 1). Between 16:00 h and 02:00 h GMT each night, sampling was restricted to surface water measurements and towed zooplankton nets while the ship undertook larger scale surveys around the position of the buoy. A storm during 7 April prevented sampling. Fig. 1 shows the 4 station positions on a SeaWiFS ocean colour composite of images collected between 2 and 14 April 2002.

Water samples were collected with a rosette of $24 \times 20 \text{ dm}^3$ Niskin sampling bottles fitted with a Seabird CTD, oxygen sensor, fluorometer and transmissometer. The daily sampling programme involved an intensive 'pre-dawn' sampling period between 02:00 h and 05:00 h GMT for zooplankton net hauls, a vertically resolved chemistry and plankton biomass CTD, a euphotic zone CTD for productivity estimates derived from 24 h incubations and depth profiles using FRRF. This was followed by a second sampling period between 10:00 h and 13:00 h GMT for a vertically resolved chemistry and plankton biomass CTD, a euphotic zone CTD for productivity estimates derived from 2 h incubations and FRRF profiles. At Stn 7 only, FRRF profiles were also collected at 09:00 h and 16:00 h GMT each day.

Nutrients. Dissolved inorganic nutrient concentrations were analysed using a segmented flow autoanalyser within 2 h of collection. Silicate was determined according to Kirkwood (1989), and nitrate was measured following the procedure of Brewer & Riley (1965).

Dissolved oxygen. Dissolved oxygen was measured using an automated Winkler titration system with a photometric endpoint, and chemical reagents based on Carritt & Carpenter (1966) ($450 \text{ g MnSO}_4 \cdot 4\text{H}_2\text{O dm}^{-3}$, $320 \text{ g NaOH} + 600 \text{ g NaI dm}^{-3}$, $280 \text{ cm}^3 \text{ H}_2\text{SO}_4 \text{ dm}^{-3}$). Oxygen saturation was calculated from the equations for the solubility of oxygen in seawater of Benson & Krause (1984).

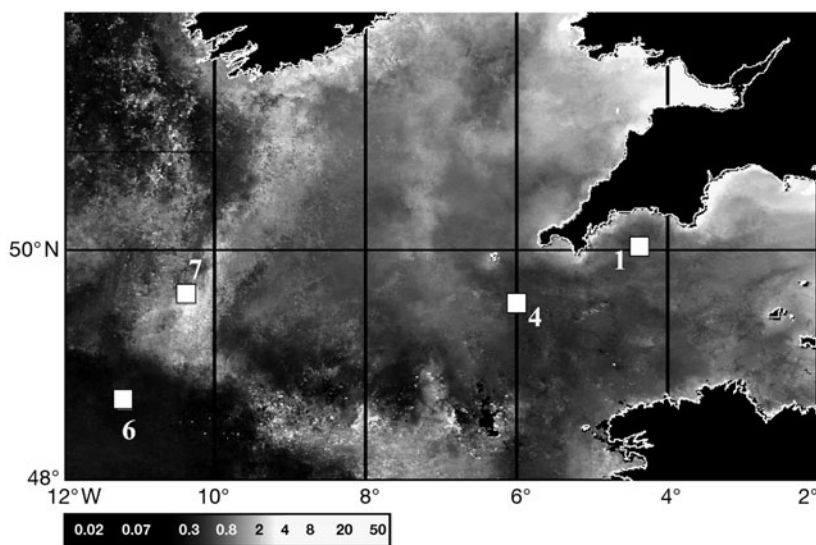


Fig. 1. Positions of the sampling stations presented on a SeaWiFS ocean colour composite of images collected between 2 and 14 April 2002. Bar shows chl *a* in mg m^{-3} . SeaWiFS data courtesy of NASA

Table 1. Hydrographic and biogeochemical characteristics of the sampling stations (temperature [$^{\circ}\text{C}$], chl *a* [mg m^{-3}], inorganic nutrients [mmol m^{-3}] and community composition [cells cm^{-3}] are the means of values in the surface 10 m). Numbers after decimal point in the station code represent the event number; nd: not determined

Day in April 2002	Station	Depth of 1% surface irradiance (m)	Mean daily PAR (W m^{-2})	Water temp. ($^{\circ}\text{C}$)	Chl <i>a</i> (mg m^{-3})	$a_{\text{CDOM}}(440)$ (m^{-1})	Nitrate (mmol m^{-3})	Silicate (mmol m^{-3})	<i>Synechococcus</i> ($\text{cells} \times 10^3 \text{ cm}^{-3}$)	Picoeukaryotes ($\text{cells} \times 10^3 \text{ cm}^{-3}$)	Centric diatoms (cells cm^{-3})	Heterotrophic bacteria ($\text{cells} \times 10^5 \text{ cm}^{-3}$)
2	1.02	30	163.9	10.6	1.13	0.055	4.38	1.71	11.5	7.8	0.1	5.0
3	4.02	30	208.5	10.7	0.59	0.106	5.84	3.79	6.1	3.5	0.4	3.5
5	6.08	55	143.5	12.0	0.36	0.046	6.91	3.49	37.7	21.6	2.5	5.1
6	7.07	40	144.5	11.2	1.82	0.037	4.06	0.61	3.2	56.7	59.8	6.2
8	7.21	40	208.3	11.3	3.51	0.046	4.00	0.54	1.9	16.4	588.7	7.9
9	7.37	40	203.8	11.4	3.45	0.043	3.50	0.05	0.8	7.1	1011.0	6.5
10	7.55	35	163.4	11.5	4.22	0.042	1.87	0.30	0.6	7.5	1807.9	7.7
11	7.72	35	153.6	11.5	3.09	0.042	2.11	0.60	0.9	11.7	775.1	10.4
12	7.90	35	210.5	11.5	nd	0.085	2.56	nd	0.6	5.8	nd	9.0

Plankton community structure. Seawater samples (250 cm³) were collected pre-dawn for the enumeration of microphytoplankton. Samples were preserved in acid Lugol's solution (2% final concentration) and stored in cool, dark conditions until analysis in the laboratory by settlement microscopy. Sub-samples (50 cm³) were concentrated by sedimentation for >72 h, and all cells between 10 and 200 µm were identified and enumerated at 320× magnification (Widdicombe et al. 2002).

Seawater samples for enumeration of phytoplankton and heterotrophic bacteria were collected from the 'pre-dawn' CTD in clean 250 cm³ polycarbonate bottles. Samples for phytoplankton analysis were stored at 4°C in the dark and analysed on board within 2 h. All analyses were carried out using a Becton Dickinson FACSort™ flow cytometer equipped with an air-cooled laser providing blue light at 488 nm. Besides counting the cells, the flow cytometer also measured chlorophyll fluorescence (>650 nm), phycoerythrin fluorescence (585 ± 21 nm), green fluorescence (530 ± 15 nm) and side scatter (light scattered at 90° to the laser beam). Data acquisition was triggered on chlorophyll fluorescence. The flow rate of the flow cytometer was calibrated daily using Beckman Coulter Flowset fluorospheres of known concentration. Measurements of light scatter and fluorescence were made using CellQuest software (Becton Dickinson) with log amplification on a 4 decade scale with 1024 channel resolution. Bivariate scatter plots of phycoerythrin against chlorophyll fluorescence were used to discriminate *Synechococcus* spp. from the other phytoplankton, based on their phycoerythrin fluorescence. Pico-phytoplankton were discriminated based on a combination of side scatter and chlorophyll fluorescence. Bacterial samples were fixed with paraformaldehyde (1% final concentration), left at 4°C in the dark for 24 h, and frozen at –80°C until post-cruise analysis. These samples were thawed at room temperature and then stained with Sybr Green I DNA stain (1% of commercial concentration) and potassium citrate (300 mM) in the ratio 100 sample:1 Sybr Green I:9 potassium citrate for 1 h at room temperature in the dark. Samples were analysed on the flow cytometer for 1 to 2 min at a flow rate of ca. 40 µl min⁻¹. Bacteria were enumerated using a combination of side scatter and green fluorescence from the Sybr Green I.

Phytoplankton pigments, photosynthetic pigment specific absorption coefficients and coloured dissolved organic material. Pigments were extracted from GF/F filtered phytoplankton by placing filters in 2 cm³ methanol containing an internal standard apocarotenolate (Sigma-Aldrich) and sonicating using an ultrasonic probe (30 s, 50 W). Extracts were centrifuged to remove filter and cell debris (2147 × *g*,

5 min) and analysed using reversed-phase HPLC (Hypersil 3 mm C8 MOS-2) with gradient elution, as described by Barlow et al. (1997), using Thermo-Separations instrumentation with photo-diode array spectroscopy (PDA) and Chrom-Quest software. Pigments were identified using retention time and spectral match using PDA (Jeffrey et al. 1997), and pigment concentrations were calculated using response factors generated from calibrations against a suite of pigment standards (DHI Water and Environment).

The absorption coefficients of total particulate and detrital material retained on GF/F filters were measured before and after pigment extraction using NaClO 1% active chloride from 350 to 750 nm at a 1 nm bandwidth using a dual beam Hitachi U-3310 spectrophotometer retro-fitted with a spectralon coated integrating sphere, following the methods of Tassan & Ferrari (1995).

Replicate seawater samples were filtered through 0.2 µm Whatman Nuclepore membrane filters using acid-cleaned glassware. The first dm³ of filtrate was discarded, before collecting a 0.5 dm³ sample. This sample was refrigerated until analysis, which occurred within 4 h (Mitchell et al. 2000). The absorption properties of the coloured dissolved organic material (CDOM) in the sample were determined in 10 cm quartz cuvettes from 200 to 850 nm relative to a bi-distilled MilliQ reference blank using the spectrophotometer described above. $a_{\text{CDOM}}(\lambda)$ was calculated from the optical density of the sample and the cuvette path length. Further details of these measurement protocols can be found in Tilstone et al. (2004) at: http://envisat.esa.int/workshops/mavt_2003/MAVT-2003_802_REVAMPprotocols3.pdf.

Primary production derived from ¹⁴C incubations. 24 h simulated in situ incubations — PP (¹⁴C_{SIS}): Water from each of 8 depths was sub-sampled into 3 clear 60 cm³ polycarbonate bottles and 1 opaque 60 cm³ polycarbonate bottle; all bottles were pre-cleaned following JGOFS protocols (IOC 1994), to reduce trace metal contamination. Each sample was inoculated with 370 kBq (10 µCi) NaH¹⁴CO₃ and transferred to an on-deck incubation system for 24 h. Neutral density and blue filters were used to simulate subsurface irradiance at the sample depths corresponding to 97, 55, 33, 20, 14, 7, 3 and 1% of the surface irradiance and were maintained at surface temperature by pumping sea water from a depth of ~7 m through the incubator. After incubation, the suspended material in each sample was filtered sequentially through 5 and 0.2 µm polycarbonate filters at a vacuum pressure of <40 cm Hg. The filters were then exposed to concentrated HCl fumes for 5 min, dried over silica gel and the ¹⁴C activity determined on board in order to estimate the daily rate of organic carbon fixation.

Spectral photosynthesis–irradiance (PE) incubations — PP ($^{14}\text{C}_{\text{PUR}}$): Photosynthesis–irradiance experiments were conducted at 10:00 h GMT each day. Fourteen subsamples in 125 cm³ polycarbonate bottles were inoculated with between 185 kBq (5 μCi) and 370 kBq (10 μCi) of ^{14}C -labelled bicarbonate and incubated in photosynthesetrons for 2 h. Full details of the incubator design and methods can be found in Tilstone et al. (2003). The daily integrated primary production (PP($^{14}\text{C}_{\text{PUR}}$), mmol C m⁻² d⁻¹) was estimated using a bio-optical model which inputs E_{PUR} , chl a and spectral photosynthetic parameters calculated from measurements of $a_{\text{ph}}(\lambda)$ (phytoplankton absorption coefficient) following:

$$\text{PP}({}^{14}\text{C}_{\text{PUR}}) = \int_{t=0}^{24} \int_{z=0}^{z_{1\%}} \text{Chl } a(z) P_m^B(z) [1 - \exp(-E_{\text{PUR}}(t, z)/E_{K(\text{PUR})}(z))] dz dt \quad (1)$$

where t is time, z is depth, P_m^B is the maximum photosynthetic rate, E_K is the light saturation parameter and PUR is photosynthetic useable radiation.

Integrated primary production derived from remote sensing algorithms. Two satellite models were used to estimate primary production. Each model can be operated using satellite derived variables (ocean colour or sea surface temperature, SST) and meteorological data from models or satellites; however, to test model capability and to compare satellite model estimates with *in situ* primary production, we used *in situ* values of chl a and irradiance derived from the Case 1 in-water light field.

Vertical generalised production model: Integrated primary production (PP_(VGP_M)) was derived from the VGP model of Behrenfeld & Falkowski (1997):

$$\text{PP}_{(\text{VGP}_M)} = 0.66125 P_{\text{opt}}^B [E_0/(E_0 + 4.1)] Z_{\text{eu}} C_{\text{opt}} D_{\text{irr}} \quad (2)$$

where P_{opt}^B is the optimum rate of chlorophyll specific carbon fixation in the water column, Z_{eu} is the depth of the 1% light level, C_{opt} is the chlorophyll concentration at P_{opt}^B , E_0 is surface daily photosynthetic active radiation (PAR) and D_{irr} is the photoperiod irradiance. Z_{eu} was computed from chl a following the relationships of Morel & Berthon (1989). P_{opt}^B was derived from a photoacclimation model based on mean daily irradiance over the water column and a knowledge of whether the phytoplankton assemblage is nutrient replete or deplete (Behrenfeld et al. 2002).

Wavelength resolving algorithm: Integrated primary production [PP_(M91)] was also derived from the wavelength resolving algorithm of Morel (1991):

$$\sum \text{PP}_{(\text{M91})} = 12 a_{\text{max}}^* \phi_m \int_0^{Z_{\text{eu}}} \int_0^{700} \int_0^{400} \text{Chl } a(z) \text{PUR}(z, t, \lambda) f(x(z, t)) d\lambda dz dt \quad (3)$$

implemented following Smyth et al. (2005) and Tilstone et al. (2005). The maximum quantum yield for

growth (ϕ_m) and the maximum phytoplankton chl a -specific absorption coefficient (a_{max}^*) were parameterised using chl a following Morel et al. (1996). The above water light field was computed from Gregg & Carder (1990). Integration was performed over all daylight hours, from 400 to 700 nm, to the 1% light level and computed through the iterative approach of Morel & Berthon (1989). The model was run using surface chl a and temperature assuming a homogeneous water column profile of chl a , a_{max}^* and ϕ_m .

Oxygen gross production, net community production and community respiration. Oxygen gross production (GP), net community production (NCP), daily oxygen uptake (DOU) and dark community respiration (DCR) were determined from 2 light/dark incubation techniques: (1) the change in dissolved oxygen and (2) ^{18}O production from H_2^{18}O and changes in O_2/Ar ratios. Net community production was also derived from *in situ* changes in dissolved oxygen corrected for air-sea exchange.

In vitro dissolved oxygen flux: Water samples (25 dm³) were collected into acid-washed opaque polypropylene aspirators from depths equivalent to 97, 55, 33, 14, 3 and 1% of surface irradiance. Water was siphoned from each aspirator into 60 cm³ borosilicate glass bottles. From each depth, 4 zero time replicates were fixed immediately, and a further 8 replicate bottles were incubated for 24 h in the same surface water cooled light and dark simulated *in situ* incubators as described above for PP($^{14}\text{C}_{\text{SIS}}$). Production and respiration rates were calculated from the difference between the means of the quadruplicate light and dark incubated and zero time analyses, and are reported with an associated SE. The median coefficient of variation (CV = [SD × 100]/mean) of the zero, dark and light analyses were 0.09 (n = 64), 0.13 (n = 64) and 0.2% (n = 45), respectively. The mean of the SEs of the DCR(O_2) and NCP(O_2) rate measurements were 0.29 mmol O_2 m⁻³ d⁻¹ (n = 64) and 0.54 mmol O_2 m⁻³ d⁻¹ (n = 45), respectively. Data are available as part of a global database at <http://web.pml.ac.uk/amt/data/respiration.xls> (Robinson & Williams 2005) GP(O_2), NCP(O_2) and DCR(O_2) were converted into units of carbon using a photosynthetic quotient (PQ) and respiratory quotient (RQ) of 1.2 and 0.8, respectively.

Incubations with H_2^{18}O : The method of Bender et al. (1987) was used with modifications as described by Luz et al. (2002). Samples were collected into duplicate 120 cm³ quartz glass bottles from the same 6 depths as for GP(O_2) described above. H_2^{18}O (~0.3 g of 98%) was added to the samples before incubation in the same simulated *in situ* incubators used for PP($^{14}\text{C}_{\text{SIS}}$) and GP(O_2). At the end of the 24 h incubation, water samples were drawn into 300 cm³ pre-evacuated gas extraction vessels (with Louwers Hapert[®] O-ring stop-

cocks) containing 1 cm³ of a HgCl₂ saturated solution to prevent any biological activity, and carefully stored for later analysis.

In the laboratory, the water and headspace in the sampling flasks were equilibrated for 24 h at room temperature, and after equilibration the water was evacuated leaving headspace gases with only a very small fraction of the original water. $\delta^{18}\text{O}$ of O₂ and oxygen:argon (O₂/Ar) ratios in the remaining gas were determined according to the procedure of Barkan & Luz (2003). O₂ and Ar were purified from other gases and transferred to stainless steel holding tubes for further mass spectrometric measurements. $\delta^{18}\text{O}$ of O₂ and the O₂/Ar ratio in the purified O₂-Ar mixture were measured by dual inlet mass spectrometry on a Thermo Finnigan DELTA^{plus} instrument. The analytical precision (SE) of $\delta^{18}\text{O}$ and $\delta\text{O}_2/\text{Ar}$ measurements was 0.01 and 0.1 ‰, respectively. The $\delta^{18}\text{O}$ of the spiked water samples was determined by the CO₂ equilibration method. In order to avoid contamination of the mass spectrometer with highly ¹⁸O-enriched CO₂ (~1500 ‰), the spiked water was diluted (approximately 1:50) with distilled water of known isotopic composition. This dilution was taken into account in the calculation of the $\delta^{18}\text{O}$ of the spiked water samples. The $\delta^{18}\text{O}$ of CO₂ equilibrated with diluted spiked water, was measured using a Gas Bench II/DELTA-^{plus}XL MS with precision better than 0.1 ‰.

Gross production, GP(¹⁸O), was calculated using the equation of Luz et al. (2002):

$$\text{GP}^{(18\text{O})} = \frac{[\text{O}_2]_{\text{fin}} \times (\delta^{18}\text{O}_{\text{fin}} - \delta^{18}\text{O}_{\text{avg}} - \epsilon_R) - [\text{O}_2]_{\text{in}} \times (\delta^{18}\text{O}_{\text{in}} - \delta^{18}\text{O}_{\text{avg}} - \epsilon_R)}{\delta^{18}\text{O}_w - \delta^{18}\text{O}_{\text{avg}} - \epsilon_R} \quad (4)$$

where [O₂]_{in} and [O₂]_{fin} are the initial and final O₂ concentrations (mmol m⁻³), respectively; $\delta^{18}\text{O}_w$ is the $\delta^{18}\text{O}$ of the spiked sea water (‰); $\delta^{18}\text{O}_{\text{in}}$ and $\delta^{18}\text{O}_{\text{fin}}$ are the initial and final $\delta^{18}\text{O}$ of dissolved O₂ (‰), respectively; and $\delta^{18}\text{O}_{\text{avg}} = (\delta^{18}\text{O}_{\text{in}} + \delta^{18}\text{O}_{\text{fin}})/2$. The fractionation factor ϵ_R represents discrimination due to O₂ uptake in the bottle. Variations in this factor up to ± 20 ‰ do not significantly affect the calculated GP(¹⁸O), and in the present study, we used ϵ_R of -21.6 ‰ (Luz et al. 2002). [O₂]_{in} was determined by Winkler titration of a sample collected directly from the Niskin bottle immediately after sampling for the H₂¹⁸O incubations. [O₂]_{fin} was calculated from [O₂]_{in} and the initial and final $\delta\text{O}_2/\text{Ar}$ values from equations given by Luz et al. (2002). Net community production [NCP($\delta\text{O}_2/\text{Ar}$)] was calculated from [O₂]_{fin} - [O₂]_{in}, and daily oxygen uptake [DOU(¹⁸O, $\delta\text{O}_2/\text{Ar}$)] was calculated as GP(¹⁸O) - NCP($\delta\text{O}_2/\text{Ar}$) (Luz et al. 2002). DOU was also calculated from DOU(¹⁸O, O₂) = GP(¹⁸O) - NCP(O₂) for comparative purposes (Grande et al. 1989b, Dickson & Orchardo 2001). GP(¹⁸O), NCP($\delta\text{O}_2/\text{Ar}$) and DOU were converted into

carbon units using a PQ or RQ of 1.2 or 0.8, respectively. No attempt was made to correct for Mehler reaction or photorespiration.

Net community production derived from *in situ* dissolved oxygen flux: Seawater samples were collected from 12 depths within the upper 120 m of the water column from the pre-dawn casts. Samples were siphoned directly from the Niskin sampling bottle into 100 cm³ borosilicate glass bottles. Each bottle was rinsed and then carefully flushed with at least 200 cm³ of sample water. Samples were fixed with Winkler reagents and titrated as described above. The change in *in situ* dissolved oxygen was calculated from the increase in the depth integrated oxygen inventory at Stn 7 for the 3 d when temperature and salinity determinations suggested that sampling had taken place within the same water mass (see below). Oxygen inventories were calculated by trapezoidal integration for the upper 35 m. This depth was chosen as (1) it was equivalent to the euphotic zone, (2) it was below the mixed layer and (3) below this depth, oxygen concentrations were decreasing, i.e. respiration was greater than photosynthesis. As some of the oxygen produced by photosynthesis would be lost to the atmosphere by gas exchange, the measured change in upper ocean dissolved oxygen was corrected for gas flux in order to derive net community production. This flux was calculated from the product of the transfer velocity and the concentration gradient of oxygen between the atmosphere and seawater. The wind speed at 10 m height under neutral air boundary conditions was derived from wind speed, air temperature, water temperature and relative humidity measured with an *in situ* anemometer positioned at 16.4 m above sea level, using the equations of Large & Pond (1981, 1982) as described by Nightingale et al. (2000). The transfer velocity was calculated from the relationship of Nightingale et al. (2000) and a Schmidt number of 943 appropriate for oxygen at 11.3°C using the equations of Wanninkhof (1992). The atmosphere/seawater oxygen concentration gradient was calculated from the difference between measured dissolved oxygen in the surface layer and that predicted from solubility equations at *in situ* temperature and salinity (Benson & Krause 1984).

Gross production derived from FRRF. A Chelsea Instruments FAST-TRACKA FRR fluorometer with dual 'Light' and 'Dark' chambers was used to measure active fluorescence. The FRRF was used with an acquisition sequence of 100 saturation flashes, 20 relaxation flashes and 10 ms sleep time between acquisitions; the flash duration was set to 1.34 μs . Light (L) and dark (D) chambers produced independent measurements of F_L , F_D , F_{mL} , F_{mD} (arbitrary units, $m = \text{maximum}$), the operating efficiency of photosystem II,

$\Delta F'/F_m' = (F_{mL} - F_L)/F_{mL}$ (dimensionless), the cross-section for photosystem II, $\sigma_{\text{PSII,L,D}}$ ($10^{-20} \text{ m}^2 \text{ photon}^{-1}$) and a turnover time of electron transfer, τ_L , τ_D (μs). Depth (m) and *in situ* irradiance (PAR; $\mu\text{mol quanta m}^{-2} \text{ s}^{-1}$) were logged with each FRR fluorescence acquisition on each cast. The FRR fluorometer was attached to an optical profiler with the LED array facing horizontally. Seawater blanks were taken and found to be negligible. Casts were performed at dawn and then at intervals (typically every 2 to 4 h) throughout the day. Quality control of data was performed using the methodology of Smyth et al. (2004) and the data for each parameter binned into 2 m depth bins using a median filter.

The calculation of the instantaneous depth and time dependent value of gross production using FRRF has been described by Smyth et al. (2004):

$$\text{GP}_{\text{FRRF}}(z) = 1.87 \times 10^{-4} \Delta F'/F_m'(z) \sigma_{\text{PSII}}(\text{max}) E_{\text{PAR}}(z) \text{Chl } a(z) \quad (5)$$

where $\text{GP}_{\text{FRRF}}(z)$ is in units of $\text{mmol C m}^{-3} \text{ h}^{-1}$; σ_{PSII} is the effective cross section of photosystem II ($10^{-20} \text{ m}^2 \text{ photon}^{-1}$) and is the maximum value observed when non-photochemical quenching is negligible, $\Delta F'/F_m'$ is the operating efficiency of PSII under ambient light (unitless); E_{PAR} is the photosynthetically active radiation ($\mu\text{mol photons m}^2 \text{ s}^{-1}$); and $\text{Chl } a(z)$ is the depth dependent chl *a* concentration (mg m^{-3}). This equation assumes 4 photons are delivered to photosystem II reaction centres (RCII) per O_2 evolved, that the maximum value of $\Delta F'/F_m'$ equals 0.65 and is obtained when all RCII are functional and operating at maximum efficiency, that n_{PSII} is 500 mol chl *a* RCII $^{-1}$, and that the photosynthetic quotient is 1.2.

Data from a particular depth at each of the profiles on a particular day were integrated to calculate GP_{FRRF} at each depth ($\text{mmol C m}^{-3} \text{ d}^{-1}$). These values were then integrated for the water column above the 1% light depth to give euphotic zone depth integrated GP_{FRRF} in $\text{mmol C m}^{-2} \text{ d}^{-1}$.

Mathematical and statistical analysis. As each method is subject to measurement error, comparisons between the various methods were derived from model II reduced major axis (RMA) regressions. However, in order to predict $\text{GP}^{(18\text{O})}$ and $\text{GP}(\text{O}_2)$ from $\text{PP}^{(14\text{C}_{\text{SIS}})}$, the ordinary least squares (OLS) linear regression model of \log_{10} transformed data was used. One-way analysis of variance (ANOVA) of \log_{10} transformed data are given as $F_{1,108} = x$, $p = y$, where F is the mean square to mean square error ratio, subscripts denote the degrees of freedom and p is the ANOVA critical significance value. Stepwise multiple regression was employed on normal distributed data to assess the variation in integrated production in relation to other biogeochemical parameters. Volumetric measurements of $\text{PP}^{(14\text{C}_{\text{SIS}})}$, $\text{GP}^{(18\text{O})}$, $\text{GP}(\text{O}_2)$, $\text{NCP}(\Delta\text{O}_2)$, $\text{NCP}(\text{O}_2)$, $\text{DCR}(\text{O}_2)$,

$\text{DOU}^{(18\text{O}, \text{O}_2)}$ and $\text{DOU}^{(18\text{O}, \delta\text{O}_2/\text{Ar})}$ were integrated to the depth of 1% of surface irradiance using trapezoidal integration.

RESULTS

Hydrography and plankton community

The hydrographic and biogeochemical characteristics of each sampling station measured at 04:00 h GMT each day are summarised in Table 1. Stn 1 was located at the geographic position of Stn E1, a long-term time series station situated ca. 40 km southwest of Plymouth, UK, in ~70 m of water. At the time of sampling, the water column was completely mixed to 70 m, with a temperature of 10.6°C and a chl *a* concentration of $\sim 1 \text{ mg m}^{-3}$. The autotrophic community was dominated by picoplankton. Stn 4 was located on the continental shelf in 105 m of water. Mean surface water chl *a* concentration was 0.6 mg m^{-3} , again dominated by picoautotrophs, and inorganic nutrient concentrations were relatively high ($5.8 \text{ mmol NO}_3 \text{ m}^{-3}$ and $3.8 \text{ mmol Si m}^{-3}$). The 'off-shelf' station (water depth 2375 m), Stn 6, had the lowest chl *a* concentration ($< 0.4 \text{ mg m}^{-3}$), the highest *Synechococcus* abundance ($38 \times 10^3 \text{ cells cm}^{-3}$), the highest surface temperature (12.0°C), the deepest euphotic zone (depth of 1% surface irradiance) and the highest surface nitrate concentration ($6.9 \text{ mmol NO}_3 \text{ m}^{-3}$).

Stn 7, on the Great Sole Bank (water depth 147 m), was first sampled on 6 April 2002. Surface temperature was 11.2°C, surface chl *a* was 1.8 mg m^{-3} and the silicate concentration was depleted to $0.6 \text{ mmol Si m}^{-3}$. The water was thermally stratified at 80 m, and the euphotic zone encompassed the upper 40 m. Picoeukaryote abundance was the highest seen during the study at $57 \times 10^3 \text{ cells cm}^{-3}$ and the phytoplankton was dominated by centric diatoms such as *Rhizosolenia* spp., *Chaetoceros* spp. and *Thalassiosira* spp. A near-gale during the night of 6–7 April 2002 (17 m s^{-1} , east-northeast) completely mixed the water column to 120 m. When sampling resumed at 02:00 h GMT on 8 April 2002, the chl *a* concentration was 3.5 mg m^{-3} , picoeukaryote abundance was $16 \times 10^3 \text{ cells cm}^{-3}$ and the abundance of centric diatoms was $588 \text{ cells cm}^{-3}$. At 04:00 h GMT on 9 April, surface silicate concentration was $0.05 \text{ mmol Si m}^{-3}$, and the abundance of centric diatoms was $1011 \text{ cells cm}^{-3}$ (equivalent to a biomass of 138 mg C m^{-3}). At 04:00 h GMT on 10 April, the centric diatom abundance had almost doubled to $1807 \text{ cells cm}^{-3}$ alongside an increase in chl *a* concentration to 4.2 mg m^{-3} . The surface silicate concentration was 0.3 mmol m^{-3} . Twenty-four hours later, chl *a* concentration was 3 mg m^{-3} , picoeukaryote abundance had in-

creased to 12×10^3 cells cm^{-3} and the abundance of centric diatoms had decreased to 775 cells cm^{-3} . The abundance of heterotrophic bacteria, which had remained between 6.2 and 7.9×10^5 cells cm^{-3} between 6 and 10 April, was now 10.4×10^5 cells cm^{-3} .

The temperature and salinity in the surface 35 m at Stn 7, sampled at 04:00 h GMT each day between 9 and 12 April 2002, varied by 0.133°C (11.412 to 11.545°C) and 0.007 salinity units (35.585 to 35.592 salinity units). The temperature and salinity in the surface 35 m at Stn 7 during 5 and 6 April, prior to the storm, ranged from 11.196 to 11.249°C and from 35.515 to 35.555 salinity units. Surface temperature and salinity during the underway surveys around the ARGOS buoy between 10 and 12 April varied from 10.82 to 11.58°C and from 35.39 to 35.61 salinity units. Therefore, the limited variability in temperature and salinity between 9 and 12 April compared to that seen between 10 and 12 April in the vicinity of Stn 7 but not alongside the ARGOS buoy, and the difference between the temperature and salinity at Stn 7 before and after the storm, suggested that sampling at 04:00 h GMT each day between 9 and 12 April 2002 had been within the same or a very similar water mass (Fig. 2). Using continuous SST and conductivity data, Llewellyn et al.

(2008) also came to the conclusion that vertical profiles collected at 04:00 h GMT at Stn 7 each day between 8 and 12 April 2002 were from the same or a very similar water mass.

Estimates of production and respiration

Depth profiles of primary and gross production are shown in Fig. 3 for Stns 4, 6 and 7 where more than 4 methods were used. Surface water $\text{GP}(\text{O}_2)$ ranged from 1 to 4 $\text{mmol C m}^{-3} \text{d}^{-1}$ at Stns 1, 4 and 6 where pico-autotrophs were dominant and increased from 8 to 33 $\text{mmol C m}^{-3} \text{d}^{-1}$ between the 6 and 11 April at Stn 7 when diatoms were dominant. Depth integrated rates of $\text{GP}(\text{O}_2)$ ranged more than 20-fold between Stn 4 on 3 April ($31 \text{ mmol C m}^{-2} \text{d}^{-1}$) and Stn 7 on 10 April ($700 \text{ mmol C m}^{-2} \text{d}^{-1}$; Table 2). At Stn 7, depth integrated $\text{GP}(\text{O}_2)$ increased $\sim 20\%$ between 8 and 9 April, $\sim 15\%$ between 9 and 10 April and decreased $\sim 35\%$ between 10 and 11 April 2002. Surface water dark community respiration [$\text{DCR}(\text{O}_2)$] ranged from $0.6 \text{ mmol C m}^{-3} \text{d}^{-1}$ at Stn 6 to $2.5 \text{ mmol C m}^{-3} \text{d}^{-1}$ at Stn 7 on 10 April when chl *a* concentration and $\text{GP}(\text{O}_2)$ also reached their maxima. The magnitude of $\text{DCR}(\text{O}_2)$

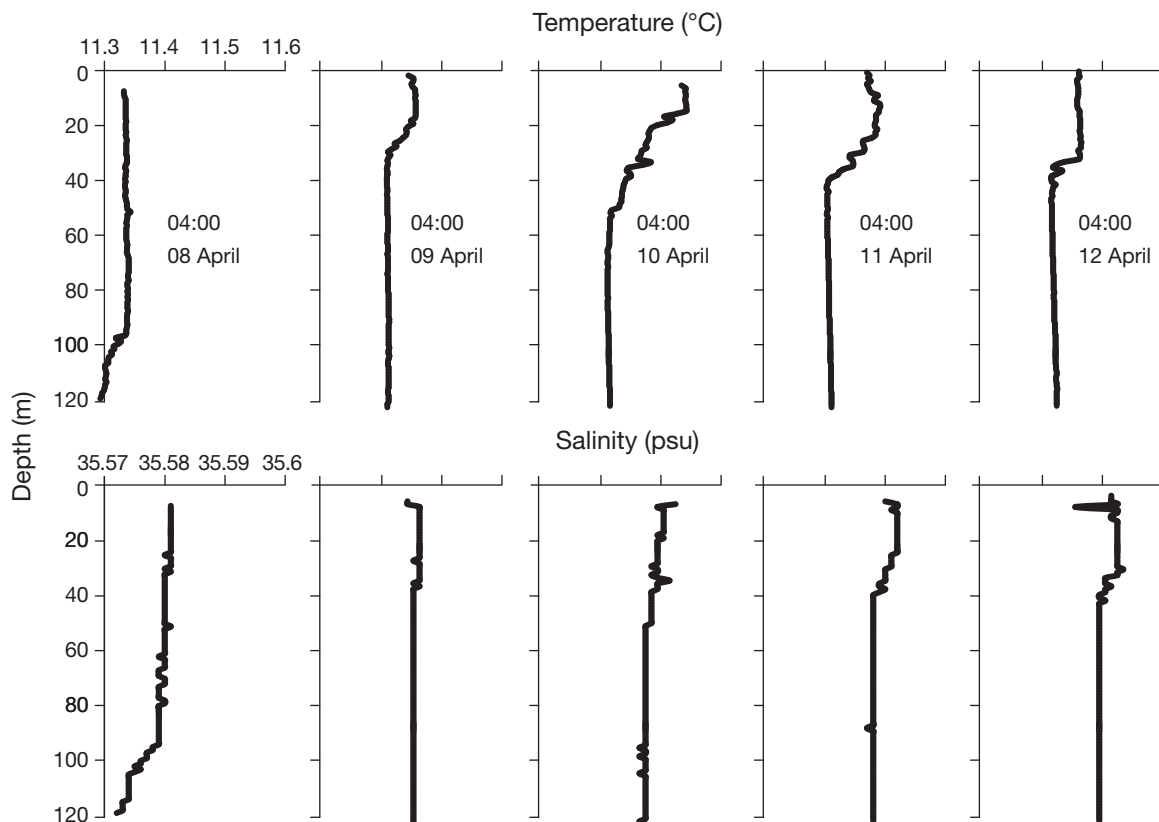


Fig. 2. Temperature and salinity depth profiles at Stn 7 sampled at 04:00 h GMT each day between 8 and 12 April 2002

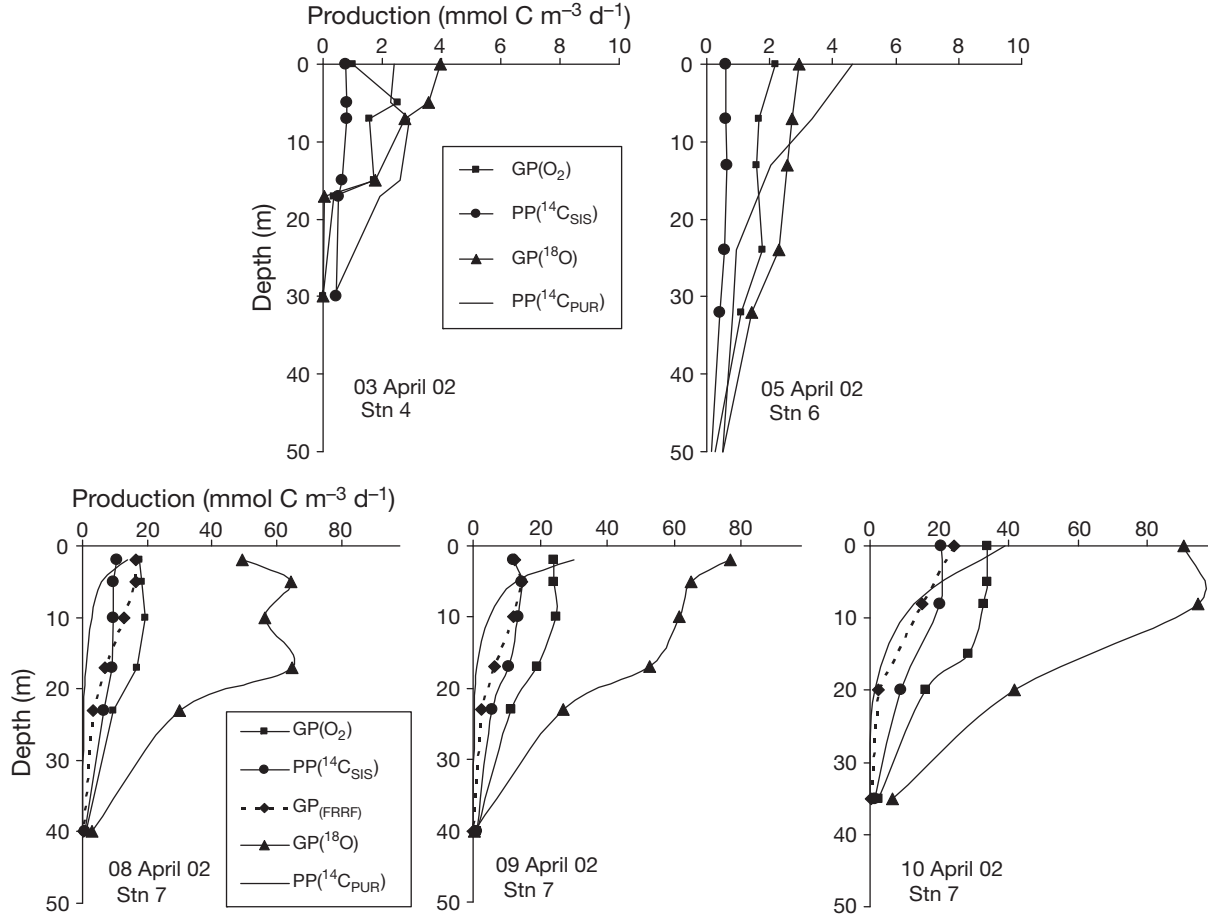


Fig. 3. Depth profiles of primary production — $PP^{14}C_{SIS}$ and $PP^{14}C_{PUR}$ — and gross production — $GP(O_2)$, $GP^{18}O$ and $GP_{(FRRF)}$ — at Stns 4, 6 and 7. See Table 2 for abbreviations

as a percentage of the magnitude of $GP(O_2)$ ranged from 55 % at Stn 4, ~35 % at Stns 1 and 6, ~20 % at Stn 7 on 6 April and ~10 % at Stn 7 between 8 and 11 April.

Depth integrated $PP^{14}C_{SIS}$ ranged from ~20 $mmol\ C\ m^{-2}\ d^{-1}$ ($0.24\ g\ C\ m^{-2}\ d^{-1}$) at Stns 1, 4 and 6 to > 400 $mmol\ C\ m^{-2}\ d^{-1}$ ($4.8\ g\ C\ m^{-2}\ d^{-1}$) on 10 April at Stn 7 (Table 2). $PP^{14}C_{SIS}$ was on average 47 % lower than $GP(O_2)$ and 36 % lower than $NCP(O_2)$. One-way ANOVA of the volumetric data ($mmol\ C\ m^{-3}\ d^{-1}$) showed a significant difference between $GP(O_2)$ and $PP^{14}C_{SIS}$ ($F_{1,84} = 3.94$, $p = 0.047$) and no significant difference between $NCP(O_2)$ and $PP^{14}C_{SIS}$ ($F_{1,84} = 0.38$, $p = 0.541$). The relationship between the volumetric measurements of these 3 production estimates in units of $mmol\ C\ m^{-3}\ d^{-1}$ can be described by: $PP^{14}C_{SIS} = 0.61 \times GP(O_2) - 0.30$ ($r^2 = 0.99$, $n = 38$); $\log PP^{14}C_{SIS} = 0.90 \times \log GP(O_2) - 0.18$ ($r^2 = 0.95$, $n = 38$) and $PP^{14}C_{SIS} = 0.64 \times NCP(O_2) + 0.21$ ($r^2 = 0.99$, $n = 38$); $\log PP^{14}C_{SIS} = 0.99 \times \log NCP(O_2) - 0.18$ ($r^2 = 0.96$, $n = 32$), respectively. One-way ANOVA of the volumetric data ($mmol\ C\ m^{-3}\ d^{-1}$) also showed a significant difference between $GP(O_2)$ and $PP^{14}C_{PUR}$ ($F_{1,83} = 8.44$, $p = 0.005$)

and no significant difference between $NCP(O_2)$ and $PP^{14}C_{PUR}$ ($F_{1,83} = 1.88$, $p = 0.174$). There was no significant difference between $PP^{14}C_{SIS}$ and $PP^{14}C_{PUR}$ (1-way ANOVA of all volumetric data, $F_{1,75} = 0.76$, $p = 0.385$), and the relationship between the volumetric measurements is described by: $PP^{14}C_{SIS} = 0.78 \times PP^{14}C_{PUR} + 2.28$ ($r^2 = 0.63$, $n = 39$) and $\log PP^{14}C_{SIS} = 0.99 \times \log PP^{14}C_{PUR} + 0.16$ ($r^2 = 0.51$, $n = 37$). However, depth integrated $PP^{14}C_{SIS}$ was on average 48 % lower than depth integrated $PP^{14}C_{PUR}$ at Stns 1, 4 and 6 and an average 84 % higher than depth integrated $PP^{14}C_{PUR}$ at Stn 7.

Depth integrated $GP^{18}O$ ranged from 49 $mmol\ C\ m^{-2}\ d^{-1}$ at Stn 4 to 2003 $mmol\ C\ m^{-2}\ d^{-1}$ on 10 April at Stn 7. $GP^{18}O$ was an average 2.4 times the magnitude of $GP(O_2)$ and 4.5 times the magnitude of $PP^{14}C_{SIS}$. The volumetric data were related according to $GP^{18}O = 3.03 \times GP(O_2) - 1.63$ ($r^2 = 0.99$, $n = 27$); $\log GP^{18}O = 1.23 \times \log GP(O_2) + 0.16$ ($r^2 = 0.92$, $n = 27$) and $GP^{18}O = 5.25 \times PP^{14}C_{SIS} - 0.43$ ($r^2 = 0.98$, $n = 28$); $\log GP^{18}O = 1.38 \times \log PP^{14}C_{SIS} + 0.39$ ($r^2 = 0.90$, $n = 28$). Predictive OLS regressions of log transformed data between

Table 2. Daily production and respiration estimates ($\text{mmol C m}^{-2} \text{d}^{-1}$) integrated to the depth of 1% surface irradiance. Oxygen-based rate measurements were converted into carbon units using photosynthetic and respiratory quotients of 1.2 and 0.8, respectively. nd: not determined. PP: primary production; SIS: simulated *in situ*; PUR: photo-synthetic useable radiation; VGPM/M91: 2 remote sensing algorithms; GP: gross production; NCP: net community production; FRRF: fast repetition rate fluorometry; DCR: Dark community respiration; DOU: daily oxygen uptake

Day in April 2002	Station	PP($^{14}\text{C}_{\text{SIS}}$) \pm SE	PP($^{14}\text{C}_{\text{PUR}}$)	PP(VGPM)	PP(M91)	GP(^{18}O) \pm SE	GP(O_2) \pm SE	GP(FRRF)	NCP(O_2) \pm SE	DCR(O_2) \pm SE	DOU ($^{18}\text{O}, \text{O}_2$)
2	1.02	24 \pm 2	26	99	149	nd	68 \pm 11	nd	41 \pm 10	26 \pm 10	nd
3	4.02	18 \pm 1	48	59	112	49 \pm 2	31 \pm 9	nd	13 \pm 5	17 \pm 7	36
5	6.08	24 \pm 1	89	55	91	99 \pm 4	66 \pm 12	nd	44 \pm 13	21 \pm 10	55
6	7.07	nd	159	114	325	nd	195 \pm 11	282	158 \pm 14	36 \pm 7	nd
8	7.21	269 \pm 24	138	209	276	1604 \pm 32	479 \pm 25	246	423 \pm 24	55 \pm 8	1181
9	7.37	327 \pm 27	223	269	327	1572 \pm 77	595 \pm 24	278	519 \pm 22	73 \pm 9	1053
10	7.55	414 \pm 32	281	252	231	2003 \pm 42	700 \pm 20	178	633 \pm 17	65 \pm 7	1370
11	7.72	304 \pm 17	123	163	273	nd	442 \pm 23	nd	379 \pm 22	61 \pm 8	nd
12	7.90	nd	189	174	235	nd	nd	nd	nd	nd	nd

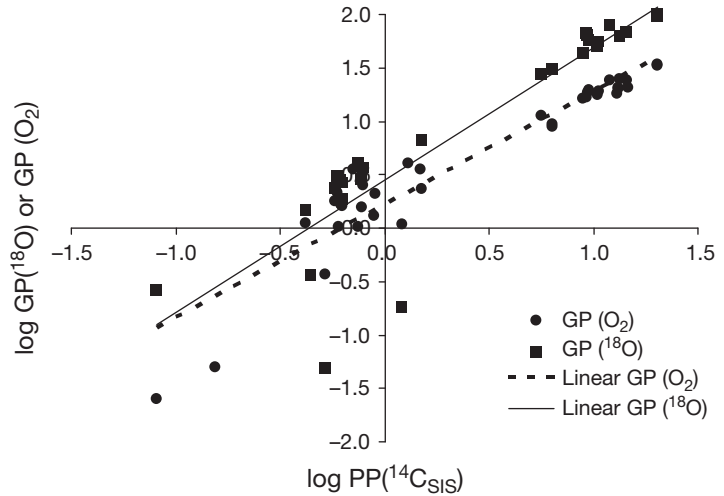


Fig. 4. Relationship between PP ($^{14}\text{C}_{\text{SIS}}$) and each of GP(O_2) and GP(^{18}O). Lines are the ordinary least squares (OLS) regression equations $\log \text{GP}(^{18}\text{O}) = 1.24 \times \log \text{PP}(^{14}\text{C}_{\text{SIS}}) + 0.45$ ($r^2 = 0.8$) and $\log \text{GP}(\text{O}_2) = 1.06 \times \log \text{PP}(^{14}\text{C}_{\text{SIS}}) + 0.22$ ($r^2 = 0.9$). See Table 2 for abbreviations

GP(O_2) and PP($^{14}\text{C}_{\text{SIS}}$) and GP(^{18}O) and PP($^{14}\text{C}_{\text{SIS}}$) (all in $\text{mmol C m}^{-3} \text{d}^{-1}$) are given in Fig. 4.

Volumetric net community production derived from light/dark bottle changes in O_2/Ar [$\text{NCP}(\delta\text{O}_2/\text{Ar})$] and O_2 concentrations [$\text{NCP}(\text{O}_2)$] were related by the regression equation $\text{NCP}(\delta\text{O}_2/\text{Ar}) = 0.85 \times \text{NCP}(\text{O}_2) - 2.52$ ($r^2 = 0.97$; $n = 28$). Daily oxygen uptake rates determined from GP(^{18}O) - $\text{NCP}(\delta\text{O}_2/\text{Ar})$ and from GP(^{18}O) \times $\text{NCP}(\text{O}_2)$ were related by the regression equation $\text{DOU} (^{18}\text{O}, \text{O}_2) = 1.09 \times \text{DOU} (^{18}\text{O}, \text{O}_2) + 2.03$ ($r^2 = 0.99$; $n = 28$). Daily oxygen uptake rates calculated from the difference between GP(^{18}O) and NCP(O_2) [$\text{DOU} (^{18}\text{O}, \text{O}_2)$] (e.g. Grande et al. 1989b, Dickson & Orchardo 2001) were on average 12-fold greater than 24 h rates of DCR(O_2), suggesting substantial rates of oxygen uptake in the light. This ratio decreased with depth and was 8-fold higher at Stn 7,

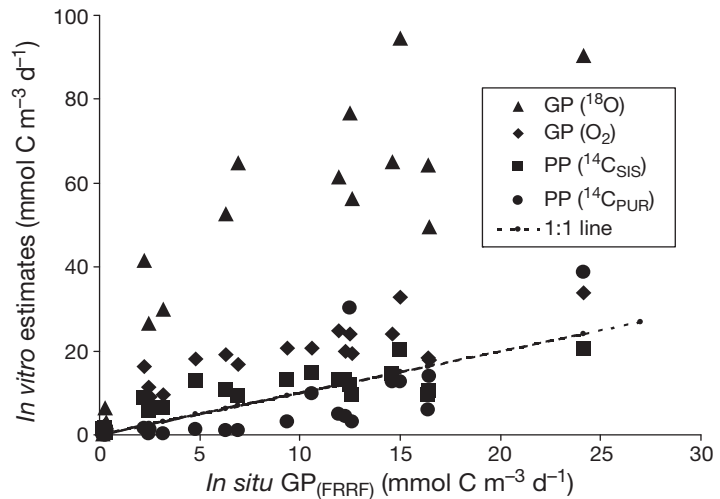


Fig. 5. Relationship between *in vitro* estimates of production—GP(O_2), GP(^{18}O), PP($^{14}\text{C}_{\text{SIS}}$), PP($^{14}\text{C}_{\text{PUR}}$)—and an *in situ* (GP(FRRF)) estimate of production. See Table 2 for abbreviations

which was dominated by diatoms, than at the stations where picoautotrophs dominated.

Depth integrated gross production derived from *in situ* FRRF [$GP_{(FRRF)}$] was on average 27 % lower than $PP^{14}C_{SIS}$, 59 % lower than $GP(O_2)$, 86 % lower than $GP^{18}O$ and 47 % higher than $PP^{14}C_{PUR}$ (Table 2). There was no significant difference between $GP_{(FRRF)}$ and $PP^{14}C_{SIS}$ ($F_{1,43} = 1.15$, $p = 0.290$) or between $GP_{(FRRF)}$ and $PP^{14}C_{PUR}$ ($F_{1,41} = 1.31$, $p = 0.259$). Fig. 5 shows the relationship between the volumetric measurements of $GP(O_2)$, $GP^{18}O$, $PP^{14}C_{SIS}$ and $PP^{14}C_{PUR}$ in relation to the 1:1 line with $GP_{(FRRF)}$.

Fig. 6 shows the change in *in situ* dissolved oxygen between 04:00 h GMT on 8 April and 04:00 h GMT on 11 April. Fig. 2 shows an increase in temperature (0.12°C) and salinity (0.004 salinity units) between 04:00 h GMT on 8 April and 04:00 h GMT on 9 April presumably due to the storm mixed surface layer warming and re-stratifying. However, this could also be indicative of different water masses being sampled. *In situ* oxygen inventories were therefore only calculated between 04:00 h GMT on 9 April and 04:00 h GMT on 12 April. The depth integrated (to 35 m) change in dissolved oxygen ranged from an increase of 1725 mmol $O_2 m^{-2}$ on 9 April to a decrease of 176 mmol

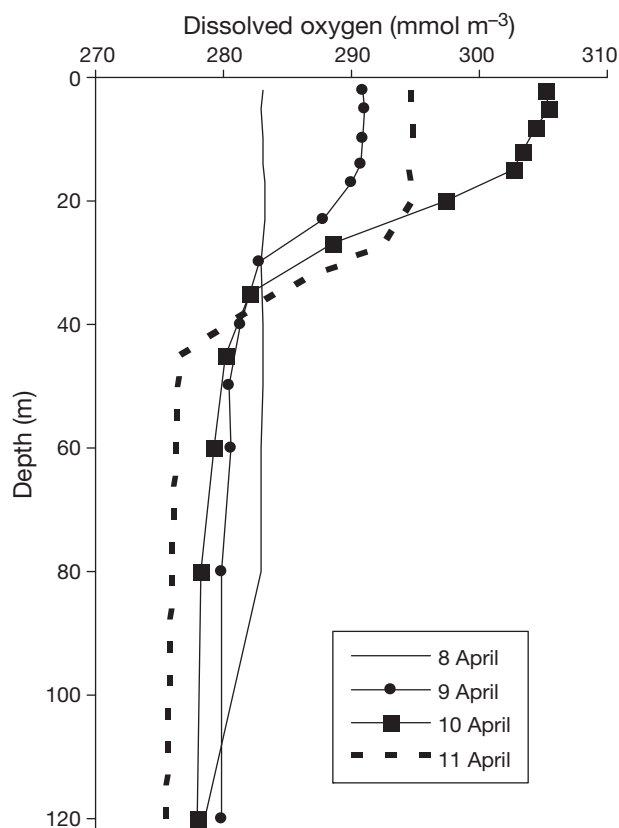


Fig. 6. Depth profiles of dissolved oxygen at Stn 7 between 8 and 11 April 2002

$O_2 m^{-2}$ on 11 April, with a mean increase of 467 mmol $O_2 m^{-2} d^{-1}$. Surface oxygen saturation reached a maximum of 112 % at 04:00 h GMT on 10 April, decreasing to 108 % at 04:00 h GMT on 11 April and 106 % at 04:00 h GMT on 12 April. The mean wind speed during the study was $3.4 \pm 1.2 ms^{-1}$, the concentration gradient of oxygen between the atmosphere and surface seawater ranged from 10 to 30 mmol $O_2 m^{-2}$, and the oxygen evasion calculated from the relationship of Nightingale et al. (2000) ranged from 10 to 25 mmol $O_2 m^{-2} d^{-1}$. The mean net community production derived from changes in *in situ* dissolved oxygen corrected for air–sea exchange [$NCP(\Delta O_2)$] was 484 mmol $O_2 m^{-2} d^{-1}$. The mean $NCP(O_2)$ derived from *in vitro* oxygen changes for the same 3 d was 510 mmol $O_2 m^{-2} d^{-1}$, a difference of ~5%. However, the daily air–sea exchange corrected NCPs(ΔO_2) were 1742, -131 and -159 mmol $O_2 m^{-2} d^{-1}$ compared to a daily $NCP(O_2)$ of 519, 633 and 379 mmol $O_2 m^{-2} d^{-1}$, a maximum difference of more than 3-fold.

Depth integrated primary production estimated using the satellite algorithms of Behrenfeld & Falkowski (1997) ($PP_{(VGPM)}$) and Morel (1991) ($PP_{(M91)}$) were higher than $PP^{14}C_{SIS}$ at the stations dominated by picoautotrophs — average $PP_{(VGPM)}:PP^{14}C_{SIS}$ of 3.2 and average $PP_{(M91)}:PP^{14}C_{SIS}$ of 5.4 — and lower than $PP^{14}C_{SIS}$ at the station dominated by diatoms — average $PP_{(VGPM)}:PP^{14}C_{SIS}$ of 0.7 and average $PP_{(M91)}:PP^{14}C_{SIS}$ of 0.8. The average $PP_{(VGPM)}:PP_{(M91)}$ ratio for all data was 0.68. The average difference between each of $PP_{(VGPM)}$ and $PP_{(M91)}$ and $PP^{14}C_{PUR}$ was 32 and 41 %, respectively.

DISCUSSION

Spring bloom dynamics at the Celtic Sea shelf edge

Stn E1 (part of the UK contribution to the International Council for the Exploration of the Sea, ICES, programme) has been a monitoring station since 1903 (Southward et al. 2005). Time series measurements of temperature, chl *a*, primary production and phytoplankton community composition identify a strong seasonal cycle, with chl *a* concentrations rising from ~1 to 4 mg chl *a* m^{-3} during approximately the second week of April each year, associated with the onset of stratification and the dominance of diatoms. Measurements made during this study, on 2 April 2002, identified a completely mixed water column, and chl *a* concentrations of ~1 mg m^{-3} dominated by picophytoplankton. These measurements are therefore consistent with pre-bloom conditions at this site.

The shelf station (Stn 4) is equivalent to station M1 sampled by Joint et al. (1986), and exhibits a seasonal

cycle typified by a spring bloom dominated by diatoms in April/May. In May 1984, 60% of the $PP(^{14}C_{SIS})$ of 23 $mmol\ C\ m^{-2}\ d^{-1}$ was attributable to cells $>5\ \mu m$ and the mean daily $PP(^{14}C_{SIS})$ for the whole Celtic Sea, estimated from measurements made between July 1982 and May 1984, was 62 to 250 $mmol\ C\ m^{-2}\ d^{-1}$ and 33 $mmol\ C\ m^{-2}\ d^{-1}$ for April and May, respectively (Joint et al. 1986). The relatively low concentrations of chl *a* ($0.6\ mg\ chl\ a\ m^{-3}$), nanophytoplankton and primary production ($18\ mmol\ C\ m^{-2}\ d^{-1}$), measured here on 3 April 2002, together with the relatively high concentrations of NO_3 and Si (Table 1) suggest that this was again a pre-bloom situation.

The off-shelf station (Stn 6) was in a water depth of 2375 m and also exhibited pre-bloom conditions of low chl *a* concentration ($<0.4\ mg\ chl\ a\ m^{-3}$), low centric diatom abundance ($2.5\ cells\ cm^{-3}$), high *Synechococcus* abundance ($38 \times 10^3\ cells\ cm^{-3}$), high NO_3 and Si concentration (6.9 and $3.5\ mmol\ m^{-3}$, respectively) and low primary production [$PP(^{14}C_{SIS}) = 23\ mmol\ C\ m^{-2}\ d^{-1}$]. These biogeochemical characteristics are consistent with pre-bloom conditions measured ~2 wk later in the seasonal cycle of 1994 (16 to 19 April) at $\sim 49.25^\circ\ N\ 12.8^\circ\ W$ (Rees et al. 1999). Surface chl *a* concentrations at these analogous off-shelf stations (G1, G2, G3) were $\sim 0.5\ mg\ m^{-3}$, with almost 50% attributable to picophytoplankton. Surface nitrate concentrations were 7 to 8 $mmol\ m^{-3}$, silicate concentrations were $>2\ mmol\ m^{-3}$, diatom abundance (*Pseudonitzschia* spp. and *Thalassionema* spp.) was $\sim 4\ cells\ cm^{-3}$ and primary production [$PP(^{14}C_{SIS})$] ranged from 40 to 90 $mmol\ C\ m^{-2}\ d^{-1}$ (Rees et al. 1999).

Satellite images, continuous plankton recorder (CPR) Greenness Index and previous biogeochemical studies have shown that phytoplankton biomass peaks in the first week of April at the Great Sole Bank (Stn 7; e.g. Joint et al. 2001). In the third week of April 1984, surface chl *a* concentrations at station M4 ($\sim 49.5^\circ\ N, 11^\circ\ W$) were $12\ mg\ chl\ a\ m^{-3}$, $PP(^{14}C_{SIS})$ was 280 $mmol\ C\ m^{-2}\ d^{-1}$ (assuming a euphotic zone of 40 m; $3.4\ g\ C\ m^{-2}\ d^{-1}$) of which 80% was attributable to cells $>5\ \mu m$ and the dominant diatoms were *Thalassiosira* spp. ($750\ cells\ cm^{-3}$; Joint et al. 1986). The spring bloom in April 1994 was dominated by the diatoms *Pseudonitzschia delicatissima* ($300\ cells\ cm^{-3}$), *P. seriata* ($350\ cells\ cm^{-3}$), *Thalassionema nitzschioides* ($180\ cells\ cm^{-3}$) and *Chaetoceros* spp. ($140\ cells\ cm^{-3}$). Chl *a* concentration was $0.95\ mg\ m^{-3}$ and $PP(^{14}C_{SIS})$ peaked at $>1\ g\ C\ m^{-2}\ d^{-1}$ ($83\ mmol\ C\ m^{-2}\ d^{-1}$; Joint et al. 2001). The bloom conditions encountered in the first week of April 2002 were characterised by chl *a* concentrations from 3.09 to $4.2\ mg\ m^{-3}$, $PP(^{14}C_{SIS})$ between 270 and 415 $mmol\ C\ m^{-2}\ d^{-1}$ ($5\ g\ C\ m^{-2}\ d^{-1}$) and abundances of centric diatoms (*Rhizosolenia* spp., *Chaetoceros* spp. and *Thalassiosira* spp.) of 500 to 1800 $cells\ cm^{-3}$. The differ-

ences in chl *a* concentrations and primary production between years could be due to a combination of (1) high heterogeneity on small spatial scales (see Fig. 1), (2) large changes in production on small temporal scales (Rees et al. 1999; Table 2), (3) use of satellite images and shipboard underway measurements in April 2002 to direct sampling to regions of highest primary production, and (4) the effect of the storm on 7 April 2002 in mixing nutrients back into the euphotic zone. The rates of $PP(^{14}C_{SIS})$ measured during the present study were 30% higher than $PP(^{14}C_{SIS})$ measured previously in this region; however, they are not thought to be exceptional or unrepresentative of the shelf ecosystem.

Comparison of measurements of gross and primary production

'There exists perhaps no single method or series of observations that is going to provide oceanographers with an absolute measure of primary production in the ocean. All methods, all approaches, are approximations, and thus various methods have to be combined in any measurement programme' (Marra 2002, p. 81). Several studies have combined more than 2 *in vitro* or *in situ* methods of determining marine primary production (Bender et al. 1987, 1992, 1999, 2000, Grande et al. 1989a, Kiddon et al. 1995, Dickson & Orchardo 2001, Dickson et al. 2001, Suggett et al. 2001, Marra 2002, Juraneck & Quay 2005, Sarma et al. 2005); however, only 2 of these encompass anything close to the range of chl *a* concentrations (0.36 to $4.20\ mg\ chl\ a\ m^{-3}$), primary production (18 to $414\ mmol\ C\ m^{-2}\ d^{-1}$, 200 to $5000\ mg\ C\ m^{-2}\ d^{-1}$) and phytoplankton communities (both picoplankton and diatom dominated) seen in the present study. Table 3 summarises the published comparisons of production estimates.

$PP(^{14}C_{SIS})$ versus $PP(^{14}C_{PUR})$

The average difference between depth integrated $PP(^{14}C_{SIS})$ and $PP(^{14}C_{PUR})$ was 68%. However, while the average $PP(^{14}C_{SIS}):PP(^{14}C_{PUR})$ ratio was 0.52 at Stns 1, 4 and 6, it was an average 1.84 during the diatom bloom at Stn 7. The reasons for this are unclear.

Exactly matching the spectral quality of natural sunlight in a deck or artificial light incubator is notoriously difficult, and previous discrepancies between short term photosynthetic incubations, day length deck incubations and *in situ* measurements have been attributed to this problem (e.g. Grande et al. 1989a, Lohrenz 1993, Boyd et al. 1997). Lohrenz (1993) collated data from 9 studies (1963 to 1992) comparing ^{14}C

Table 3. Primary, gross and net community production as ^aa fraction of GP(¹⁸O), ^ba fraction of PP(¹⁴C), ^ca fraction of PP(¹⁴C_{PE}) or PP(¹⁴C_{PUR}) or ^da fraction of GP(O₂) using a photosynthetic quotient (PQ) of ^e1.0, ^f1.1, ^g1.2, ^h1.25, ⁱ1.4 or ^j1.5. GP(¹⁸O) was corrected by ^k0%, ^l10%, ^m15% or ⁿ20% for photorespiration and Mehler reaction. nd: not determined, '?': not given in publication; MERL: Marine Ecosystem Research Laboratory of the University of Rhode Island, USA. See Table 2 for abbreviations

GP (¹⁸ O)	PP (¹⁴ C _{SIS})	PP (¹⁴ C _{PE}) (¹⁴ C _{PUR})	GP (O ₂)	GP (Pump probe)	GP (FRRF)	GP (Δ ¹⁷ O)	Site	Source
1 ^{e,k}	0.6–1.0 ^a	nd	1 ^a	nd	nd	nd	MERL mesocosms	Bender et al. (1987)
1 ^{h,k}	0.3–0.5 ^a	nd	0.5 ^a	nd	nd	nd	North Pacific Gyre	Grande et al. (1989a)
1 ^{e,k}	0.4 ^a	nd	nd	nd	nd	nd	North Atlantic	Bender et al. (1992), Kiddon et al. (1995)
1 ^{g,k}	0.4 ^a	nd	nd	nd	nd	nd	Equatorial Pacific	Bender et al. (1999), their Table 1
1 ^{h,n}	0.3–0.6 ^a	nd	nd	nd	nd	nd	Arabian Sea	Laws et al. (2000)
1 ^{h,k}	0.4–0.5 ^a	nd	nd	nd	nd	nd	Arabian Sea	Dickson et al. (2001)
1 ^{g,k}	0.5–0.7 ^a	nd	nd	nd	nd	0.9–2.8 ^a	North Pacific Gyre	Juranek & Quay (2005)
1 ^{h,k}	nd	nd	0.7 ^a	nd	nd	nd	Ross Sea	Bender et al. (2000)
1 ^{h,k}	nd	nd	0.6 ^a	nd	nd	nd	Florida Shelf	Hitchcock et al. (2000)
1 ⁱ	nd	nd	0.3–0.9 ^a	nd	nd	nd	Antarctic Polar Front	Dickson & Orchardo (2001)
nd	1 ^j	nd	1.4–2.2 ^b	nd	nd	nd	Coastal Antarctic	Aristegui et al. (1996)
nd	1 ^e	nd	1.2–2.4 ^b	nd	nd	nd	Coastal Antarctic	Robinson et al. (1999)
nd	1 ^h	nd	2.6 ^b	nd	nd	nd	Atlantic Ocean	Robinson et al. (2002)
nd	1 ^f	nd	2.0 ^b	nd	nd	nd	North Sea	Rees et al. (2002)
nd	1 ^e	nd	0.5–1.8 ^b	nd	nd	nd	North Pacific Gyre	Williams et al. (2004)
nd	1 ⁱ	?	nd	nd	1.3 ^b	nd	UK shelf sea	Moore et al. (2003)
nd	1 ^g	nd	nd	nd	0.5–1.3 ^b	nd	UK shelf sea	Smyth et al. (2004)
nd	nd	1 ^g	nd	1.1 ^c	nd	nd	NW Atlantic Ocean	Kolber & Falkowski (1993)
nd	nd	1 ^g	nd	0.7 ^c	nd	nd	NE Atlantic Ocean	Boyd et al. (1997)
nd	nd	1 ^e	nd	nd	2.0 ^c	nd	North Atlantic Ocean	Suggett et al. (2001)
nd	nd	nd	1	nd	0.9–1.4 ^d	1.1–2.2 ^d	Sagami Bay, Japan	Sarma et al. (2005)
1 ^{g,k}	0.2 ^a	0.1–1.0 ^a	0.3–0.7 ^a	nd	0.2 ^a	nd	UK shelf sea	This study
	1	0.4–3.7 ^b	2.0 ^b	nd	0.4–0.9 ^b	nd	UK shelf sea	This study
		1	2.2 ^c	nd	1.4 ^c	nd	UK shelf sea	This study
			1	nd	0.3–1.4 ^d	nd	UK shelf sea	This study

PP derived from *in situ* incubations (IS) with ¹⁴C PP derived from simulated *in situ* incubations (SIS) and ¹⁴C PP derived from photosynthesis (P) irradiance (E) curves [PP(¹⁴C_{PE})]. No systematic bias was found between PP(¹⁴C_{IS}) and PP(¹⁴C_{SIS}), with differences ranging ±80%. PE curves most often yielded estimates of PP that were higher (by up to 2-fold) than PP(¹⁴C_{IS}); however, 5 studies also measured lower rates (up to 40%) of PP(¹⁴C_{PE}) than PP(¹⁴C_{IS}). The results obtained in the present study therefore fall within the range of published studies. The apparent shift in relationship between PP(¹⁴C_{SIS}) and PP(¹⁴C_{PUR}) between stations dominated by picoautotrophs and those dominated by diatoms is difficult to explain in terms of recreating the natural light quality, since the equipment used was the same, and the mean daily natural irradiance was similar for both types of sampling station (Table 1).

PP(¹⁴C_{SIS}) samples were collected at 04:00 h GMT, whereas PP(¹⁴C_{PUR}) samples were collected at 10:00 h GMT, and even though temperature and salinity profiles indicated that there were no major differences between the water mass sampled at 04:00 h and that sampled at 10:00 h (data not shown), the heteroge-

neous nature of the bloom (Fig. 1), may have contributed to the differences seen. For example, on 11 April 2002, chl *a* concentration was 3.1 mg m⁻³ at 5 m at 04:00 h when the PP(¹⁴C_{SIS}) = 304 mmol C m⁻³ d⁻¹ sample was collected and 2.23 mg m⁻³ at 5 m at 10:00 h when the PP(¹⁴C_{PUR}) = 123 mmol C m⁻³ d⁻¹ sample was collected (data not shown). However, by contrast, on 9 April 2002 chl *a* concentration was 3.38 mg m⁻³ at 5 m at 04:00 h when the PP(¹⁴C_{SIS}) = 327 mmol C m⁻³ d⁻¹ sample was collected and 4.48 mg m⁻³ at 5 m at 10:00 h when the PP(¹⁴C_{PUR}) = 223 mmol C m⁻³ d⁻¹ sample was collected (data not shown).

One intriguing but untestable reason why rates of PP(¹⁴C_{PUR}) based on 2 h incubations were lower than PP(¹⁴C_{SIS}) based on 24 h incubations only at the station dominated by diatoms, could be related to the health of the diatoms. Low silicate concentrations and measurements of bacterial abundance and production, viral abundance and diatom pigment transformation products suggest that the *Rhizosolenia* and *Chaetoceros* spp. may have been releasing dissolved organic carbon compounds in response to silicate limitation and viral infection (Llewellyn et al. 2008).

Yacobi et al. (2007) suggested that excretion and coating of cells by extracellular polymers could restrict the diffusion of ^{14}C tracer into phytoplankton cells, thereby causing underestimates of $\text{PP}^{(14}\text{C})$ during short term incubations. Diatom mucilage was visible in the surface waters at Stn 7, and readily collected with a $<200\ \mu\text{m}$ zooplankton net haul from 6 m (C. Hughes pers. comm., Hughes et al. 2008). Microscopic analysis suggested that some of the *Thalassiosira* cells were colonial, that is, embedded in a polysaccharide matrix. Unfortunately, a large proportion of DOM is colourless, and so not included in a measurement of CDOM; $a_{\text{CDOM}}(440)$ was not higher at the diatom dominated station compared to the picoautotroph dominated station and did not peak on days when the $\text{PP}^{(14}\text{C}_{\text{SIS}}):\text{PP}^{(14}\text{C}_{\text{PUR}})$ ratio was greatest (11 April 2002; Table 2). Thus, we have some evidence that the diatoms at Stn 7 were excreting DOM, but cannot show that this limited the ^{14}C uptake.

$\text{PP}^{(14}\text{C}_{\text{SIS}})$ versus $\text{GP}(\text{O}_2)$ and $\text{NCP}(\text{O}_2)$

^{14}C assimilation tends to be less than $\text{GP}(\text{O}_2)$ by a factor of ~ 0.4 to 0.8 depending on the magnitude of respiration, whether DO^{14}C excretion was measured and which (if any) photosynthetic quotient was used (see Table 3). Measurements made during the present study conform with this pattern, with depth integrated $\text{PP}^{(14}\text{C}_{\text{SIS}})$ being on average 53% of depth integrated $\text{GP}(\text{O}_2)$ (converted with a PQ of 1.2) and the slope of the regression equation between volumetric $\text{PP}^{(14}\text{C}_{\text{SIS}})$ and $\text{GP}(\text{O}_2)$ being 0.61. During this study, at all stations except Stn 4, depth integrated $\text{PP}^{(14}\text{C}_{\text{SIS}})$ was also lower than depth integrated $\text{NCP}(\text{O}_2)$, amounting on average to 64% of depth integrated $\text{NCP}(\text{O}_2)$. This $\sim 36\%$ discrepancy could be due to a combination of uncertainty in the magnitude of the PQ to use (e.g. 1.4 rather than 1.2) and excretion of DO^{14}C , which was not measured. Using the algorithm of Teira et al. (2001) suggests that excretion could have accounted for an average of 25% of $\text{PP}^{(14}\text{C}_{\text{SIS}})$ at Stns 1, 4 and 6 and an average 7% of $\text{PP}^{(14}\text{C}_{\text{SIS}})$ at Stn 7. A similar situation was measured during an Antarctic coastal bloom of *Chaetoceros* spp. and *Thalassiosira* spp., where in 60% of the stations particulate $\text{PP}^{(14}\text{C}_{\text{SIS}})$ was less than NCP derived from *in vitro* changes in dissolved inorganic carbon [$\text{NCP}(\text{DIC})$] or $\text{NCP}(\text{O}_2)$ divided by a PQ of 1.4, by an average of 25% (Robinson et al. 1999). A significant number of $\text{PP}^{(14}\text{C}_{\text{SIS}})$ derived from 12 h incubations lay below concurrent rates of $\text{NCP}(\text{O}_2)$ measured during 4 latitudinal transects of the Atlantic Ocean (Robinson et al. 2006). Yacobi et al. (2007) attributed their average ratio of $\text{NCP}(\text{O}_2)$ to $\text{PP}^{(14}\text{C})$

(derived from 3 h *in situ* incubations) of 2.2 during November to December in Lake Kinneret to slow diffusion of the radiotracer in and out of the phytoplankton cells, possibly due to production of extracellular polymers.

Although there were differences between $\text{PP}^{(14}\text{C}_{\text{SIS}})$, $\text{PP}^{(14}\text{C}_{\text{PUR}})$ and $\text{GP}(\text{O}_2)$, multiple regression analysis (data not shown) indicated that $\text{PP}^{(14}\text{C}_{\text{SIS}})$, $\text{PP}^{(14}\text{C}_{\text{PUR}})$ and $\text{GP}(\text{O}_2)$ all co-varied with chl *a*, NO_3 , NO_2 and Si, and $\text{PP}^{(14}\text{C}_{\text{PUR}})$ and $\text{GP}(\text{O}_2)$ also co-varied with cryptophytes. Hence the same biogeochemical parameters were influencing similar production estimates.

$\text{GP}^{(18}\text{O})$ versus $\text{GP}(\text{O}_2)$ and $\text{PP}^{(14}\text{C}_{\text{SIS}})$

$\text{GP}^{(18}\text{O})$ may be a better measure of gross oxygen photosynthesis than $\text{GP}(\text{O}_2)$, since it incorporates respiratory losses throughout the natural light/dark cycle. By contrast, $\text{GP}(\text{O}_2)$ involves a 24 h dark bottle incubation and so must assume that respiration in the light and in the dark are equal. However, $\text{GP}^{(18}\text{O})$ measures all oxygen production by phytoplankton irrespective of whether this is directly linked to carbon fixation (Laws et al. 2000) and so $\text{GP}^{(18}\text{O})$ converted into carbon units using only a photosynthetic quotient will be an overestimate of gross organic carbon production. The challenge is to know, at any particular time, which of the light-related reactions are occurring and so by how much $\text{GP}^{(18}\text{O})$ overestimates carbon fixation. Oxygen consumption in aquatic organisms occurs through several metabolic pathways: respiration through the cytochrome oxidase pathway, respiration by the alternative oxidase pathway, chlororespiration, photorespiration and the Mehler reaction. The first 2 processes occur in both light and dark conditions, chlororespiration is inhibited by light and the latter 2 reactions only occur under illumination. Oxygen consumption in the light has been found to be 0.6- to 20-fold greater than oxygen consumption in the dark (Bender et al. 1987, Kana 1990, 1992, Lewitus & Kana, 1995, Grande et al. 1991, Hitchcock et al. 2000, Pringault et al. 2007), with ratios derived from $\text{GP}^{(18}\text{O})$ and $\text{GP}(\text{O}_2)$ comparisons converging on 1.5 to 2.0 in natural marine populations (Table 4). Very high oxygen uptake in the light is predicted to be due principally to stimulation of energy dissipating reactions (alternative pathway, Mehler reaction, photorespiration) and to only occur when energy is in excess, e.g. when cells are exposed to saturating light (Lewitus & Kana 1995). In the absence of measurements of oxygen uptake in the light, which is linked to carbon production, previous studies have 'corrected' estimates of $\text{GP}^{(18}\text{O})$ by a factor of minus 10 to 20% for Mehler reaction and photorespiration (Laws et al. 2000, Hendricks et al. 2004). Of the 5 published

Table 4. Ratio of daily (24 h) oxygen uptake— $\text{DOU}^{(18\text{O}, \text{O}_2)} = \text{GP}^{(18\text{O})} - \text{NCP}(\text{O}_2)$ —to 24 h dark community respiration— $\text{DCR}(\text{O}_2)$ —in natural plankton communities. NCP: net community production

$\text{DOU}^{(18\text{O}, \text{O}_2)}/\text{DCR}(\text{O}_2)$ (ratio) Mean, n range	Site (dominant autotroph)	Data used and incubation procedure	Source
7.2, 1	MERL, URI ^a mesocosms (<i>Thalassiosira</i>)	Volumetric data, samples incubated on deck	Bender et al. (1987)
5.5, 3	North Pacific Gyre	Volumetric data, samples incubated on deck	Grande et al. (1989a)
3.2–8.5			
1.3, 5	North Pacific Gyre	Volumetric data, samples incubated <i>in situ</i>	Grande et al. (1989a)
0.6–2.8			
1.9, 10	Ross Sea	Depth integrated data, samples incubated <i>in situ</i>	Bender et al. (2000)
1.0–3.7			
1.6, 3	West Florida Shelf	Depth integrated data, samples incubated <i>in situ</i>	Hitchcock et al. (2000)
1.6–1.7			
1.2, 3	Antarctic Polar Front (spring)	Depth integrated data, samples incubated on deck	Dickson & Orchardo (2001)
0.8–1.5			
2.0, 4	Antarctic Polar Front (summer)	Depth integrated data, samples incubated on deck	Dickson & Orchardo (2001)
0.9–2.5			
1.4, 1	Ross Sea	Depth integrated data, samples incubated on deck	Dickson & Orchardo (2001)
2.4, 2	Celtic Sea (picoautotrophs)	Depth integrated data, samples incubated on deck	This study
2.1–2.6			
19.0, 3	Celtic Sea (diatoms)	Depth integrated data, samples incubated on deck	This study
14.4–21.5			

^aMarine Ecosystem Research Laboratory of the University of Rhode Island, USA

comparisons of $\text{GP}^{(18\text{O})}$ and $\text{GP}(\text{O}_2)$, (see Table 3), 3 studies measured $\text{GP}(\text{O}_2):\text{GP}^{(18\text{O})}$ ratios of 0.3 to 0.6, suggesting that a 20% correction to $\text{GP}^{(18\text{O})}$ for Mehler reaction and photorespiration would still have led to a 20 to 50% overestimate of $\text{GP}(\text{O}_2)$. These authors have therefore either underestimated the range of magnitude of the Mehler reaction, or they believe that the difference between $\text{GP}^{(18\text{O})}$ and $\text{GP}(\text{O}_2)$ is due to other processes in addition to oxygen reactions that are not involved in carbon assimilation (e.g. Bender et al. 1999, 2000, Dickson et al. 2001). In the present study, the mean $\text{GP}(\text{O}_2):\text{GP}^{(18\text{O})}$ ratio for the stations dominated by picoautotrophs was 0.65, and the mean $\text{GP}(\text{O}_2):\text{GP}^{(18\text{O})}$ ratio for the station dominated by diatoms was 0.34, suggesting that respiration in the light was substantially greater than respiration in the dark, and at least twice the ~20% correction usually applied for the Mehler reaction. $\text{GP}^{(18\text{O})}$ was an average 4.5-fold greater than $\text{PP}^{(14\text{C}_{\text{SIS}})}$ —the mean $\text{PP}^{(14\text{C}_{\text{SIS}}):\text{GP}^{(18\text{O})}$ ratio was 0.30 at Stns 4 and 6 and 0.19 at Stn 7—whereas previous marine studies suggest a range of $\text{PP}^{(14\text{C}_{\text{SIS}}):\text{GP}^{(18\text{O})}$ ratios between 0.3 and 1.0 (Table 3). However, 1 study in Lake Kinneret during a diatom bloom measured $\text{PP}^{(14\text{C}_{\text{SIS}}):\text{GP}^{(18\text{O})}$ ratios as low as 0.12 (Luz et al. 2002).

One further complicating factor in comparisons of gross and net production derived from dissolved oxygen production and enhancement of the $^{18\text{O}}/^{16\text{O}}$ isotopic ratio of dissolved oxygen is the potential effect of the different composition of the incubation bottles

used. $^{18\text{O}}$ incubations are usually undertaken in quartz glass bottles (e.g. Dickson et al. 2001, Juranek & Quay 2005, this study), while dissolved oxygen incubations are commonly performed in borosilicate glass bottles (e.g. Williams & Purdie 1991, Robinson et al. 2002, Williams et al. 2004, present study). Any differential light spectral exposure of the 2 sets of incubations could cause greater photoinhibition of photosynthesis and greater photochemical consumption of oxygen in the quartz bottles due to a higher transmission of UV-A and -B radiation. Both of these processes would cause an underestimate of net and gross production derived from $^{18\text{O}}$ incubations. However, in the present study, incubations of both borosilicate and quartz bottles occurred under polycarbonate screens incorporating blue and neutral density acrylic. These polycarbonate screens are opaque to wavelengths below 400 nm and above 700 nm and so reduce any effects related to these wavelengths.

Fig. 3 suggests that photoinhibition of photosynthesis may have occurred during the simulated surface incubations on 8 and 10 April at Stn 7—surface $\text{GP}^{(18\text{O})}$ is 20 and 4% lower than $\text{GP}^{(18\text{O})}$ at 5 and 8 m respectively while concomitant surface chl *a* is 7% higher than that at 5 and 8 m. We have no direct evidence to corroborate or refute whether photochemical consumption of oxygen was occurring. Published rates of non-biological oxygen consumption range from ~1 to 3 $\text{mmol O}_2 \text{ m}^{-3} \text{ d}^{-1}$ (Obenosterer et al. 2001, 2005) i.e. <2 to 3% of the surface $\text{GP}^{(18\text{O})}$ photosynthetic

rates measured here. Assuming the photochemical consumption of oxygen during the present study to be of the same order as that measured by Obernosterer et al. (2001, 2005), then the resultant underestimate of GP and NCP by GP(^{18}O) and NCP($\delta\text{O}_2/\text{Ar}$) is of lesser order (~3%) than that hypothesised to be due to photoinhibition (<20%). Underestimates of oxygen gross production due to photoinhibition of photosynthesis or photochemical consumption of oxygen are both of lesser magnitude than the overestimate of GP by GP(^{18}O) due to measurement of the Mehler reaction and photorespiration (<235%) if the entire discrepancy between GP(O_2) and GP(^{18}O) is due to only these 2 processes. In summary, differential photoinhibition and photochemistry would be minimised due to the use of polycarbonate screens, and even if 1 or both of these processes were occurring, then the estimated effect would be much less than the measured difference between GP(^{18}O) and GP(O_2).

NCP (O_2) versus NCP($\delta\text{O}_2/\text{Ar}$) and DOU (^{18}O , O_2) versus DOU(^{18}O , $\delta\text{O}_2/\text{Ar}$)

Volumetric net community production derived from light/dark bottle changes in O_2/Ar —NCP($\delta\text{O}_2/\text{Ar}$)—and O_2 concentrations—NCP(O_2)—were related by the regression equation $\text{NCP}(\delta\text{O}_2/\text{Ar}) = 0.85 \times \text{NCP}(\text{O}_2) - 2.52$ ($r^2 = 0.97$; $n = 28$). This $15 \pm 4\%$ discrepancy between NCP($\delta\text{O}_2/\text{Ar}$) measured in quartz bottles and NCP(O_2) measured in borosilicate glass bottles may be due to different light conditions of the incubations, as described above. Daily oxygen uptake rates determined from GP(^{18}O)—NCP($\delta\text{O}_2/\text{Ar}$) and from GP(^{18}O)—NCP(O_2) were related by the regression equation $\text{DOU} (^{18}\text{O}, \delta\text{O}_2/\text{Ar}) = 1.09 \times \text{DOU} (^{18}\text{O}, \text{O}_2) + 2.03$ ($r^2 = 0.99$; $n = 28$).

DOU (^{18}O , O_2) versus DCR (O_2)

Daily oxygen uptake derived from the difference between GP(^{18}O) and NCP(O_2) was 2- to 21-fold greater than DCR(O_2). For the plankton communities occurring at Stns 1, 4 and 6, the DOU(^{18}O , O_2):DCR(O_2) ratios of 2.1 and 2.6 are comparable to the range reported in the literature (Table 4); however, for the diatom bloom at Stn 7, the ratios of 14.4, 21.1 and 21.5 are 2- to 3-fold greater than the highest ratios measured before (Bender et al. 1987). Fig. 7 shows how a GP(O_2):GP(^{18}O) ratio of 0.3, measured here and in previous studies (Table 4) equates to a DOU(^{18}O , O_2):DCR(O_2) ratio of >10. Unfortunately, coupled DCR(O_2) and DOU(^{18}O , O_2) measurements have not been made in such high biomass marine diatom blooms before,

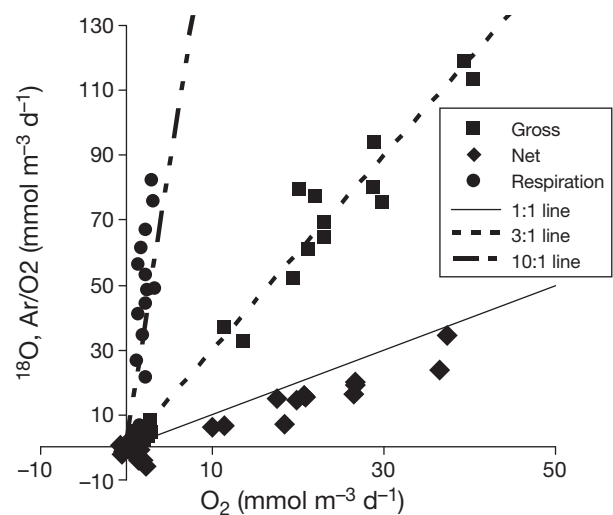


Fig. 7. Relationship between net community production, gross production and respiration derived from the dissolved oxygen and ^{18}O techniques. Rates derived from dissolved oxygen flux are plotted on the x-axis and rates derived from ^{18}O are plotted on the y-axis

and we have no measures of the factors that may have caused enhanced oxygen consumption in the light, e.g. CO_2 limitation. The high DOU(^{18}O , O_2):DCR(O_2) ratios measured here emphasise our limited knowledge of the magnitude of the various oxygen consuming processes employed by naturally occurring plankton populations. This is an area of active research (Luz et al. 2002, Pringault et al. 2007).

Without a better understanding of the range and variability of the various plankton respiration pathways it is difficult to determine whether GP(O_2) or GP(^{18}O) and DCR(O_2) or DOU(^{18}O , O_2) are the most appropriate techniques to measure plankton gross production and respiration associated with organic carbon production. If the enhanced oxygen uptake occurring in the light is only associated with the Mehler reaction and photorespiration, then GP(O_2) and DCR(O_2) are fortuitously practical methodologies (Williams & del Giorgio 2005). However, increased oxygen uptake occurring in the light may be coupled to organic carbon production either through instantaneous photo-enhancement of mitochondrial respiration and/or increased mitochondrial respiration due to increased biomass during the previous light phase and/or an increase in zooplankton/ bacterial respiration in the light (Weger et al. 1989, Bender et al. 1999, 2000, Luz et al. 2002, Hernandez-Leon & Ikeda 2005, Pace & Prairie 2005). In these situations, the magnitude of true plankton respiration would lie somewhere between that derived from DCR(O_2) and that derived from DOU(^{18}O , O_2), depending upon the rates of the various respiration pathways.

GP_(FRRF) versus PP (¹⁴C_{SIS}), PP(¹⁴C_{PUR}), GP (O₂) and GP(¹⁸O)

As far as we are aware, this is the first study to compare depth integrated GP derived from FRRF parameters with depth integrated PP and GP derived from *in vitro* O₂ and ¹⁸O incubations as well as short term PE and daylength ¹⁴C incubations. Most comparisons are between the photosynthetic parameters α^B (maximum light utilisation coefficient) and P_m^B (maximum photosynthetic rate) derived from FRRF and PP(¹⁴C_{PE}). The photosynthetic parameter α^B derived from the FRRF is reported to be 2 to 2.5 times higher than that derived from short term PP(¹⁴C_{PE}) measurements (Suggett et al. 2001, Moore et al. 2003, Smyth et al. 2004), P_m^B derived from the FRRF can be either higher (Suggett et al. 2001), lower (Smyth et al. 2004) or similar (Moore et al. 2003) to those derived from PP(¹⁴C_{PE}) incubations. Calculation of GP_(FRRF) from FRRF parameters and a biophysical model (e.g. Kolber & Falkowski 1993) allows comparisons between GP_(FRRF) and PP(¹⁴C_{PE}), PP(¹⁴C_{SIS}) and PP(¹⁴C) derived from dawn to dusk *in situ* incubations — PP(¹⁴C_{IS}) — (Moore et al. 2003, Corno et al. 2005, Melrose et al. 2006). Estimates of GP_(FRRF) and PP(¹⁴C_{SIS}) (based on 6 to 8 h incubations) in the Celtic Sea were within 10 % of each other at stratified stations and within 50 % of each other — GP_(FRRF) > PP(¹⁴C_{SIS}) — at stations with a mixed water column (Moore et al. 2003). GP_(FRRF):PP(¹⁴C_{IS}) ratios at Station ALOHA in 2002–2003 were >1.5 in near surface water and approached 1.0 deeper in the euphotic zone (Corno et al. 2005). Comparisons in Massachusetts and Narragansett Bays between GP_(FRRF) and PP(¹⁴C_{PE}) gave PP(¹⁴C_{PE}): GP_(FRRF) ratios between 0.07 and 1.44, with the most common ratio being between 0.25 and 0.35 (Melrose et al. 2006).

Since FRRF measurements allow the calculation of gross photosynthetic oxygen evolution, we would expect GP_(FRRF) to be comparable to GP(¹⁸O) and \geq PP(¹⁴C_{PUR}), PP(¹⁴C_{SIS}) and GP(O₂). However, this was not the case in the present study. GP_(FRRF) was on average 27 % lower than PP(¹⁴C_{SIS}), 59 % lower than GP(O₂), 86 % lower than GP(¹⁸O) and 47 % higher than PP(¹⁴C_{PUR}) (Table 2). These comparisons are not dissimilar to published GP_(FRRF):PP(¹⁴C_{PUR}) ratios; however, they highlight an apparent underestimate of GP_(FRRF) in relation to PP(¹⁴C_{SIS}), GP(O₂) and especially GP(¹⁸O).

Any comparison between GP_(FRRF) (derived from *in situ* measurements) and GP(O₂), GP(¹⁸O), PP(¹⁴C_{SIS}) and PP(¹⁴C_{PUR}) (derived from *in vitro* incubations) will be dependent upon how well the incubated light conditions approximate those of the natural environment, and how well 2 to 4 hourly depth profiles of FRRF measurements recreate the natural variability of light during the day (Smyth et al. 2004). In addition, sam-

ples for 24 h incubations are usually collected before sunrise, whereas GP_(FRRF) measurements are made throughout the day, hence spatial and temporal heterogeneity of samples may also contribute to differences.

However, the major uncertainty in the calculation of GP_(FRRF) is the value to use for n_{PSII} . Here and in previous studies (Falkowski 1981, Smyth et al. 2004), 500 mol chl a RCII⁻¹ was used, which is typical for eukaryotes. However, mesocosm studies have shown n_{PSII} to vary between 200 and 1200 mol chl a RCII⁻¹ (Berges et al. 1996). This could account for difference by a factor of 2 in estimates of GP_(FRRF). In the present study, using $n_{PSII} = 1000$ mol chl a RCII⁻¹ would produce GP_(FRRF):PP(¹⁴C_{SIS}) ratios between 0.8 and 1.8 and GP_(FRRF):GP(O₂) ratios between 0.5 and 1.0. This dependency upon n_{PSII} limits the ability of the FRRF to accurately determine gross production. Future research should aim to develop a method to determine *in situ* n_{PSII} .

In situ NCP(Δ O₂) versus *in vitro* NCP(O₂)

Net community production can be derived from *in situ* time series measurements of a substrate or product of photosynthesis/respiration provided that processes other than organic production, which also alter the concentrations of these substrates/products, are accounted for. In the case of dissolved oxygen, the potentially confounding processes are air–sea exchange and lateral and vertical mixing. Air–sea exchange can be estimated from a wind speed gas transfer velocity relationship and an estimate of oxygen supersaturation caused by bubble injection (0.5 to 2 %; Woolf & Thorpe 1991). Lateral and vertical mixing can be derived from inert gas tracers (Emerson et al. 1993a) or the spatial and temporal variability in salinity (Williams & Purdie 1991, Robertson & Watson 1993). The *in situ* technique was first exploited in the 1980s (e.g. Schulenberger & Reid 1981, Jenkins & Goldman 1985, Emerson 1987), and direct comparisons showed that the *in situ* and *in vitro* techniques were in general agreement. Mixed layer *in situ* CO₂ uptake was found to be ~20 % lower than, but not significantly different from, PP (¹⁴C) during a spring diatom bloom in the North Atlantic (Chipman et al. 1993, Marra 2002), the *in situ* decrease in nitrate+ammonia and phosphate was ~30 % greater than *in vitro* uptake within an eddy in the North Atlantic in June (Rees et al. 2001), and *in situ* O₂ production lay within a factor of 2 of *in vitro* ¹⁵N uptake in the subarctic Pacific (Emerson et al. 1993b). Published comparisons of *in vitro* derived NCP(O₂) with *in situ* derived NCP(Δ O₂) are given in Table 5 and range from 0.6 (Dickson & Orchardo 2001) to 5.6 (Williams & Purdie 1991). In the present study, the 3 d

Table 5. *In situ* net community production (NCP) determined from changes in dissolved oxygen, given as a ratio of *in vitro* NCP determined from bottle incubations

<i>In situ</i> NCP [NCP (ΔO_2):NCP(O_2)]	Site	Source
1–3	MERL ^a mesocosms	Bender et al. (1987)
1.6	North Atlantic	Bender et al. (1992), Kiddon et al. (1995)
0.9	Ross Sea	Bender et al. (2000)
0.6	Antarctic Polar Front	Dickson & Orchardo (2001)
5.6	North Pacific Gyre	Williams & Purdie (1991)
<3.3	UK shelf sea	This study

^aMarine Ecosystem Research Laboratory of the University of Rhode Island, USA

mean of NCP(ΔO_2) agreed with the 3 d mean of NCP(O_2) to within 5%. However, on a daily basis NCP(ΔO_2) and NCP(O_2) differed by up to 3-fold, suggesting that despite the relatively stable physical conditions at Stn 7 (Fig. 2; Llewellyn et al. 2008) advection and vertical mixing may not have been adequately accounted for.

PP_(VGPM) versus PP_(M91)

The PP_(VGPM) model was calibrated with a dataset of 1700 primary production measurements derived from *in situ* and simulated *in situ* incubations [PP($^{14}C_{IS}$) and PP($^{14}C_{SIS}$)] (Behrenfeld & Falkowski 1997); less than 3% of the calibration data were derived from PE incubations — PP($^{14}C_{PUR}$). By contrast, the PP_(M91) algorithm was calibrated with PP($^{14}C_{PUR}$) and validated using PP($^{14}C_{IS}$) (Morel 1991). Since neither model incorporates data from the present study, it is valid to use data from this study to determine which might be the most relevant model for this particular region of the Celtic Sea.

Platt & Sathyendranath (1988) showed that the choice of model is critical for accurate derivation of primary production. Platt et al. (1991) used wavelength independent and dependent models of varying complexity based on PE relationships and the irradiance field of the water column to assess their accuracy in specific regions of the North Atlantic. They found that significant errors were incurred by ignoring the spectral structure of the irradiance field and the vertical structure of the water column, which implies that PP_(M91) may be more accurate than PP_(VGPM). Carr et al. (2006), found that for estimates of global production, models based on the PP_(VGPM) algorithm consistently overestimated production compared to PP_(M91). However, although PP_(M91) was more accurate in the Mediterranean Sea and the Atlantic and Southern Oceans, the PP_(VGPM) models were more accurate in the

Pacific, Indian and Arctic Oceans. More recently, Tilstone et al. (2008), using 120 measurements of PP($^{14}C_{SIS}$) from 7 Atlantic meridional transects, found that PP_(VGPM) was more accurate in the eastern and western tropical Atlantic and that PP_(M91) was more accurate in 6 other Atlantic Ocean provinces and over the Atlantic basin as a whole.

In the present study, the average difference between PP_(VGPM) and PP_(M91) was 34%. The average PP_(VGPM):PP($^{14}C_{PUR}$) ratio was 1.36, and the average PP_(VGPM):PP($^{14}C_{SIS}$) ratio was 1.8. The average PP_(M91):PP($^{14}C_{PUR}$) ratio was 2.10, and the average PP_(M91):PP($^{14}C_{SIS}$) ratio was 2.81. At the diatom dominated station, PP_(VGPM) was an average 25% higher than PP($^{14}C_{PUR}$) and 31% lower than PP($^{14}C_{SIS}$), whereas PP_(M91) was 69% higher than PP($^{14}C_{PUR}$) and 14% lower than PP($^{14}C_{SIS}$). This suggests that PP_(VGPM), with P_{opt}^B derived from the photoacclimation model, is the more appropriate model to use for regions in the Celtic Sea with chlorophyll concentrations in the range of 3 to 4 mg m⁻³. By contrast, Tilstone et al. (2005, 2008), found that PP_(VGPM) overestimates PP in the Irish Sea and the Atlantic Ocean where the inherent optical properties of coloured dissolved organic material and suspended material also modify the light field.

CONCLUSIONS AND FUTURE WORK

In shelf sea waters dominated by picoautotrophs, 4 *in vitro* estimates of primary and gross production fell within a 3- to 4-fold range, with GP(^{18}O) > GP(O_2) > PP($^{14}C_{PUR}$) > PP($^{14}C_{SIS}$). However, in waters dominated by diatoms, 4 *in vitro* and 1 *in situ* derived estimate of PP and GP differed by up to an order of magnitude (Table 2), and GP(^{18}O) > GP(O_2) > PP($^{14}C_{SIS}$) > PP($^{14}C_{PUR}$). Consistency in equipment and approach suggests that this differential effect was not due to incubation artefacts. While many of the comparisons between any 2 of these techniques fall within previously published ranges (Tables 4 & 5), 2 anomalies occurring at the diatom dominated station are difficult to reconcile: (1) greater than 10-fold differences between uptake of dissolved oxygen in the light and in the dark, and (2) PP($^{14}C_{PUR}$) less than PP($^{14}C_{SIS}$). While both these situations have been seen before in natural and mesocosm populations (Lewitus & Kana 1995, Bender et al. 1987, Lohrenz 1993), they do not represent the currently accepted consensus.

Unfortunately, we have no way of knowing whether the enhanced oxygen consumption in the light was

only associated with processes such as the Mehler reaction, in which case estimates of gross production derived from ^{18}O incubations in diatom blooms may need to be revised downwards by more than a commonly used $\sim 20\%$ correction term (Laws et al. 2000, Hendricks et al. 2004) or whether $\text{GP}(\text{O}_2)$ and $\text{DCR}(\text{O}_2)$ need to be revised upwards to be more accurate estimates of organic carbon production.

At stations dominated by picoautotrophs, $\text{PP}(14\text{C}_{\text{SIS}}) < \text{PP}(14\text{C}_{\text{PUR}})$, whereas at the diatom dominated station, $\text{PP}(14\text{C}_{\text{SIS}}) > \text{PP}(14\text{C}_{\text{PUR}})$. The heterogeneous nature of the diatom bloom and the differences in the sampling times between $\text{PP}(14\text{C}_{\text{SIS}})$ and $\text{PP}(14\text{C}_{\text{PUR}})$ may have contributed to the differences observed. A further possibility is that dissolved organic material excreted by the diatom population under stress of silicate limitation and viral infection (Llewellyn et al. 2008) restricted the diffusion of ^{14}C into the cells (Yacobi et al. 2007) and thereby had a disproportionately larger effect on PP derived from short term incubations.

Despite more than 25 yr of active research, our understanding of the temporal and spatial variability in primary production is still incomplete. The results from the present study should stimulate investigations into the magnitude and controlling factors of light enhanced respiration and the impact that phytoplankton physiological state has on isotope flow through the cell. Such controlled physiological experiments, together with continued comparisons between *in vitro* and *in situ* methods across a range of environmental conditions and phytoplankton populations, should further constrain our estimates of marine microbial carbon production and respiration and their potential response to future environmental change.

Acknowledgements. This study forms part of the Plymouth Marine Laboratory (PML) core strategic research programme. The work could not have been completed without the professionalism and teamwork of our colleagues. Thanks are due to the Principal Scientist C. Turley, to C. Wing and E.M.S. Woodward for pre-cruise logistical organisation, to the officers and crew on board RRS 'Discovery' 261, and to P. Taylor, P. Duncan, R. Roberts and D. Young (UKORS/ RSU) for their excellent support of sampling operations. Many thanks to S. Barquero for help with ^{14}C analyses, J. Stephens for nutrient analyses, D. Cummings for chlorophyll analyses, and C. Widcombe for phytoplankton taxonomy and abundance. We are very grateful to P. Nightingale for expert advice on air-sea gas flux calculations, to T. Kana and O. Pringault for discussions on respiration in the light, to R. Torres and C. Gallienne for advice on tracking a single water mass, and to E. Laws and J. Marra for constructive reviews, which improved the quality of this manuscript. Thank you to G. Moncoiffe, C. Castellani and P. Hadziabdic at the British Oceanographic Data Centre (BODC) for providing an invaluable data management service. Fig. 1 was produced by P. Miller of the Remote Sensing Data Analysis Service at PML. SeaWiFS data courtesy of NASA.

LITERATURE CITED

- Aristegui J, Montero MF, Ballesteros S, Basterretxea G, van Lenning K (1996) Planktonic primary production and microbial respiration measured by ^{14}C assimilation and dissolved oxygen changes in coastal waters of the Antarctic Peninsula during austral summer: implications for carbon flux studies. *Mar Ecol Prog Ser* 132:191–201
- Barkan E, Luz B (2003) High precision measurements of $^{17}\text{O}/^{16}\text{O}$ and $^{18}\text{O}/^{16}\text{O}$ of O_2 and O_2/Ar ratio in air. *Rapid Commun Mass Spectrom* 17:2809–2814
- Barlow RG, Cummings DG, Gibb SW (1997) Improved resolution of mono- and divinyl chlorophylls *a* and *b* and zeaxanthin and lutein in phytoplankton extracts using reverse phase C-8 HPLC. *Mar Ecol Prog Ser* 161:303–307
- Behrenfeld MJ, Falkowski PG (1997) Photosynthetic rates derived from satellite-based chlorophyll concentration. *Limnol Oceanogr* 42:1–20
- Behrenfeld MJ, Marañón E, Siegel DA, Hooker SB (2002) Photoacclimation and nutrient-based model of light-saturated photosynthesis for quantifying oceanic primary production. *Mar Ecol Prog Ser* 228:103–117
- Bender ML, Grande K, Johnson K, Marra J and others (1987) A comparison of four methods for the determination of planktonic community metabolism. *Limnol Oceanogr* 32:1085–1098
- Bender M, Ducklow H, Kiddon J, Marra J, Martin J (1992) The carbon balance during the 1989 spring bloom in the North Atlantic Ocean, 47°N , 20°W . *Deep-Sea Res A* 39:1707–1725
- Bender M, Orchardo J, Dickson ML, Barber R, Lindley S (1999) *In vitro* O_2 fluxes compared with ^{14}C production and other rate terms during the JGOFS Equatorial Pacific experiment. *Deep-Sea Res I* 46:637–654
- Bender ML, Dickson ML, Orchardo J (2000) Net and gross production in the Ross Sea as determined by incubation experiments and dissolved O_2 studies. *Deep-Sea Res II* 47:3141–3158
- Benson BB, Krause D Jr (1984) The concentration and isotopic fractionation of oxygen dissolved in freshwater and seawater in equilibrium with the atmosphere. *Limnol Oceanogr* 29:620–632
- Berges JA, Charlebois DO, Mauzerall DC, Falkowski PG (1996) Differential effects of nitrogen limitation on photosynthetic efficiency of photosystems I and II in microalgae. *Plant Physiol* 110:689–696
- Boyd PW, Aiken J, Kolber Z (1997) Comparison of radiocarbon and fluorescence based (pump and probe) measurements of phytoplankton photosynthetic characteristics in the Northeast Atlantic Ocean. *Mar Ecol Prog Ser* 149:215–226
- Brewer PG, Riley JP (1965) The automatic determination of nitrate in seawater. *Deep-Sea Res* 12:765–772
- Campbell J, Antoine D, Armstrong R, Balch W and others (2002) Comparison of algorithms for estimating ocean primary production from surface chlorophyll, temperature and irradiance. *Glob Biogeochem Cycles* 16(3), 1035, doi 10.1029/2001GB001444
- Carr ME, Friedrichs MAM, Schmeltz M, Noguchi Aita M and others (2006) A comparison of global estimates of marine primary production from ocean color. *Deep-Sea Res II* 53:741–770
- Carritt DE, Carpenter JH (1966) Comparison and evaluation of currently employed modifications of the Winkler method for determining dissolved oxygen in seawater; a NASCO report. *J Mar Res* 24:286–319
- Chipman DW, Marra J, Takahashi T (1993) Primary produc-

- tion at 47°N and 20°W in the North Atlantic Ocean: a comparison between the ^{14}C incubation method and the mixed layer carbon budget. *Deep-Sea Res II* 40:151–169
- Corno G, Letelier RM, Abbott MR, Karl DM (2005) Assessing primary production variability in the North Pacific Subtropical Gyre: a comparison of fast repetition rate fluorometry and ^{14}C measurements. *J Phycol* 42:51–60
- Dickson ML, Orchardo J (2001) Oxygen production and respiration in the Antarctic Polar Front region during the austral spring and summer. *Deep-Sea Res II* 48:4101–4126
- Dickson ML, Orchardo J, Barber RT, Marra J, McCarthy JJ, Sambrotto RN (2001) Production and respiration rates in the Arabian Sea during the 1995 Northeast and Southwest Monsoons. *Deep-Sea Res II* 48:1199–1230
- Emerson S (1987) Seasonal oxygen cycles and biological new production in surface waters of the subarctic Pacific Ocean. *J Geophys Res* 92:6535–6544
- Emerson S, Quay P, Stump C, Wilbur D, Schudlich R (1993a) Determining primary production from the mesoscale oxygen field. *ICES Mar Sci Symp* 197:196–206
- Emerson S, Quay P, Wheeler PA (1993b) Biological productivity determined from oxygen mass balance and incubation experiments. *Deep-Sea Res I* 40:2351–2358
- Falkowski PG (1981) Light shade adaptation and assimilation numbers. *J Plankton Res* 3:203–216
- Gazeau F, Middelburg JJ, Loijens M, Vanderborgh JP, Pizay MD, Gattuso JP (2007) Planktonic primary production in estuaries: comparison of ^{14}C , O_2 and ^{18}O methods. *Aquat Microb Ecol* 46:95–106
- Grande KD, Williams PJLeB, Marra J, Purdie DA, Heinemann K, Eppley RW, Bender ML (1989a) Primary production in the North Pacific gyre: a comparison of rates determined by the ^{14}C , O_2 concentration and ^{18}O methods. *Deep-Sea Res* 36:1621–1634
- Grande KD, Marra J, Langdon C, Heinemann K, Bender M (1989b) Rates of respiration in the light measured in marine phytoplankton using an ^{18}O isotope-labeling technique. *J Exp Mar Biol Ecol* 129:95–120
- Grande KD, Bender ML, Irwin B, Platt T (1991) A comparison of net and gross rates of oxygen production as a function of light intensity in some natural plankton populations and in a *Synechococcus* culture. *J Plankton Res* 13:1–16
- Gregg WW, Carder KL (1990) A simple spectral solar irradiance model for cloudless maritime atmospheres. *Limnol Oceanogr* 35:1657–1675
- Hendricks MB, Bender ML, Barnett BA (2004) Net and gross O_2 production in the southern ocean from measurements of biological O_2 saturation and its triple isotope composition. *Deep-Sea Res I* 51:1541–1561
- Hernandez-Leon S, Ikeda T (2005) Zooplankton respiration. In: del Giorgio PA, Williams PJLeB (eds) *Respiration in aquatic ecosystems*. Oxford University Press, New York, p 57–82
- Hitchcock GL, Vargo GA, Dickson ML (2000) Plankton community composition, production, and respiration in relation to dissolved inorganic carbon on the West Florida Shelf, April 1996. *J Geophys Res* 105:6579–6589
- Holligan P, Fernandez E, Aiken J, Balch WM and others (1993) A biogeochemical study of the coccolithophore, *Emiliania huxleyi*, in the North Atlantic. *Glob Biogeochem Cycles* 7:879–900
- Hughes C, Malin G, Turley CM, Keely BJ, Nightingale PD, Liss PS (2008) The production of volatile iodocarbons by biogenic marine aggregates. *Limnol Oceanogr* 53: 867–872
- IOC (Intergovernmental Oceanographic Commission) (1994) *Protocols for the Joint Global Ocean Flux Study (JGOFS)* core measurements. UNESCO, Paris
- Jeffrey SW, Mantoura RFC, Wright SW (eds) (1997) *Phytoplankton pigments in oceanography*. UNESCO Publishing, Paris
- Jenkins WJ, Goldman V (1985) Seasonal oxygen cycling and primary production in the Sargasso Sea. *J Mar Res* 43:465–491
- Joint IR, Groom SB (2000) Estimation of phytoplankton production from space: current status and future potential of satellite remote sensing. *J Exp Mar Biol Ecol* 250:233–255
- Joint IR, Owens NJP, Pomeroy AJ (1986) Seasonal production of photosynthetic picoplankton and nanoplankton in the Celtic Sea. *Mar Ecol Prog Ser* 28:251–258
- Joint I, Wollast R, Chou L, Batten S and others (2001) Pelagic production at the Celtic Sea shelf break. *Deep-Sea Res II* 48:3049–3081
- Juranek LW, Quay PD (2005) In vitro and in situ gross primary and net community production in the North Pacific Subtropical Gyre using labeled and natural abundance isotopes of dissolved O_2 . *Glob Biogeochem Cycles* 19, GB3009, doi:10.1029/2004GB002384
- Kana TM (1990) Light-dependent oxygen cycling measured by an oxygen-18 isotope dilution technique. *Mar Ecol Prog Ser* 64:293–300
- Kana TM (1992) Relationship between photosynthetic oxygen cycling and carbon assimilation in *Synechococcus* WH7803 (Cyanophyta). *J Phycol* 28:304–308
- Karl DM, Bidigare RR, Letelier RM (2002) Sustained and aperiodic variability in organic matter production and phototrophic microbial community structure in the North Pacific Subtropical Gyre. In: Williams PJLeB, Thomas DN, Reynolds CS (eds) *Phytoplankton productivity: carbon assimilation in marine and freshwater ecosystems*. Blackwell Science, Oxford, p 222–264
- Kiddon J, Bender ML, Marra J (1995) Production and respiration in the 1989 North Atlantic Spring bloom – an analysis of irradiance dependent changes. *Deep-Sea Res I* 42: 553–576
- Kirkwood DS (1989) Simultaneous determination of selected nutrients in seawater. Copenhagen Denmark ICES C:29
- Kolber ZS, Falkowski PG (1993) Use of active fluorescence to estimate phytoplankton photosynthesis in situ. *Limnol Oceanogr* 38:1646–1665
- Large WG, Pond S (1981) Open ocean momentum flux measurements in moderate to strong winds. *J Phys Oceanogr* 11:324–336
- Large WG, Pond S (1982) Sensible and latent heat flux measurements over the ocean. *J Phys Oceanogr* 12:464–482
- Laws EA, Landry MR, Barber RT, Campbell L, Dickson ML, Marra J (2000) Carbon cycling in primary production bottle incubations: inferences from grazing experiments and photosynthetic studies using ^{14}C and ^{18}O in the Arabian Sea. *Deep-Sea Res II* 47:1339–1352
- Lewitus AJ, Kana TM (1995) Light respiration in six estuarine phytoplankton species: contrasts under photoautotrophic and mixotrophic growth conditions. *J Phycol* 31: 754–761
- Llewellyn CA, Tarran GA, Galliene CP, Cummings DG and others (2008) Microbial dynamics during the decline of a spring diatom bloom in the Northeast Atlantic. *J Plankton Res* 30:261–273
- Lohrenz SE (1993) Estimation of primary production by the simulated in situ method. *ICES Mar Sci Symp* 197:159–171
- Longhurst A, Sathyendranath S, Platt T, Caverhill C (1995) An estimate of global primary production in the ocean from satellite radiometer data. *J Plankton Res* 17:1245–1271

- Luz B, Barkan E, Sagi Y, Yacobi YZ (2002) Evaluation of community respiratory mechanisms with oxygen isotopes: a case study in Lake Kinneret. *Limnol Oceanogr* 47:33–42
- Marra J (2002) Approaches to the measurement of plankton production. In: Williams PJLeB, Thomas DN, Reynolds CS (eds) *Phytoplankton productivity: carbon assimilation in marine and freshwater ecosystems*. Blackwell Science, Oxford, p 78–108
- Melrose DC, Oviatt CA, O'Reilly JE, Berman MS (2006) Comparisons of fast repetition rate fluorescence estimated primary production and ^{14}C uptake by phytoplankton. *Mar Ecol Prog Ser* 311:37–46
- Mitchell GB, Bricaud A, Carder K, Cleveland J and others (2000) Determination of spectral absorption coefficients of particles, dissolved material and phytoplankton for discrete water samples. In: Fargion GS, Mueller JL (eds). *Ocean optics protocols for satellite ocean color sensor validation, Revision 2*. NASA Tech Memo 209966. NASA Goddard Space Flight Center, Greenbelt, MD, p 125 – 153
- Moore CM, Suggett D, Holligan PM, Sharples J and others (2003) Physical controls on phytoplankton physiology and production at a shelf sea front: a fast repetition-rate fluorometer based field study. *Mar Ecol Prog Ser* 259:29–45
- Moore CM, Suggett DJ, Hickman AE, Young-Nam K and others (2006) Phytoplankton photoacclimation and photoadaptation in response to environmental gradients in a shelf sea. *Limnol Oceanogr* 51:936–949
- Morel A (1991) Light and marine photosynthesis: a spectral model with geochemical and climatological implications. *Prog Oceanogr* 26:263–306
- Morel A, Berthon JF (1989) Surface pigments, algal biomass profiles, and potential production of the euphotic layer - relationships reinvestigated in view of remote-sensing applications. *Limnol Oceanogr* 34:1545–1562
- Morel A, Antoine D, Babin M, Dandonneau Y (1996) Measured and modelled primary production in the northeast Atlantic (EUMELI JGOFS program): the impact of natural variations in photosynthetic parameters on model predictive skill. *Deep-Sea Res I* 43:1273–1304
- Nightingale PD, Malin G, Law CS, Watson AJ and others (2000) In situ evaluation of air-sea gas exchange parameterizations using novel conservative and volatile tracers. *Glob Biogeochem Cycles* 14:373–387
- Obernosterer I, Ruardij P, Herndl GJ (2001) Spatial and diurnal dynamics of dissolved organic matter (DOM) fluorescence and H_2O_2 and the photochemical oxygen demand of surface water DOM across the subtropical Atlantic Ocean. *Limnol Oceanogr* 46:632–643
- Obernosterer I, Catala P, Reinthaler T, Herndl GJ, Lebaron P (2005) Enhanced heterotrophic activity in the surface microlayer of the Mediterranean Sea. *Aquat Microb Ecol* 39:293–302
- Pace ML, Prairie YT (2005) Respiration in lakes. In: del Giorgio PA, Williams PJLeB (eds) *Respiration in aquatic ecosystems*. Oxford University Press, New York, p 103–121
- Platt T, Sathyendranath S (1988) Oceanic primary production: estimation by remote sensing at local and regional scales. *Science* 241:1613–1620
- Platt T, Caverhill C, Sathyendranath S (1991) Basin-scale estimates of oceanic primary production by remote sensing - the North Atlantic. *J Geophys Res* 96:15147–15159
- Pringault O, Tassas V, Rochelle-Newall E (2007) Consequences of respiration in the light on the determination of production in pelagic systems. *Biogeosciences* 4:105–114
- Rees AP, Joint I, Donald KM (1999) Early spring bloom phytoplankton-nutrient dynamics at the Celtic Sea Shelf Edge. *Deep-Sea Res I* 46:483–510
- Rees AP, Joint I, Woodward EMS, Donald KM (2001) Carbon, nitrogen and phosphorus budgets within a mesoscale eddy: comparison of mass balance with in vitro determinations. *Deep-Sea Res II* 48: 859–872
- Rees AP, Woodward EMS, Robinson C, Cummings DG, Tarran GT, Joint I (2002) Size-fractionated nitrogen uptake and carbon fixation during a developing coccolithophore bloom in the North Sea during June 1999. *Deep-Sea Res II* 49:2905–2927
- Robertson JE, Watson AJ (1993) Estimation of primary production by observation of changes in the mesoscale carbon dioxide field. *ICES Mar Sci Symp* 197:207–214
- Robinson C, Williams PJLeB (2005) Respiration and its measurement in surface marine waters. In: del Giorgio PA, Williams PJLeB (eds) *Respiration in aquatic ecosystems*. Oxford University Press, New York p147–180
- Robinson C, Archer SD, Williams PJLeB (1999) Microbial dynamics in coastal waters of East Antarctica: plankton production and respiration. *Mar Ecol Prog Ser* 180: 23–36
- Robinson C, Serret P, Tilstone G, Teira E, Zubkov MV, Rees AP, Woodward EMS (2002) Plankton respiration in the Eastern Atlantic Ocean. *Deep-Sea Res I* 49:787–813
- Robinson C, Poulton AJ, Holligan PM, Baker AR and others (2006) The Atlantic Meridional Transect Programme (AMT): a contextual view 1995–2005. *Deep-Sea Res II* 53: 1485–1515
- Sarma VVSS, Abe O, Hashimoto S, Hinuma A, Saino T (2005) Seasonal variations in triple oxygen isotopes and gross oxygen production in the Sagami Bay, central Japan. *Limnol Oceanogr* 50:544–552
- Schulenberg E, Reid J (1981) The Pacific shallow oxygen maximum, deep chlorophyll maximum, and primary productivity reconsidered. *Deep-Sea Res* 28:901–919
- Smyth TJ, Pemberton KL, Aiken J, Geider RJ (2004) A methodology to determine primary production and phytoplankton photosynthetic parameters from fast repetition rate fluorometry. *J Plankton Res* 26:1337–1350
- Smyth TJ, Tilstone GH, Groom SB (2005) Primary production estimates from satellite data using a coupled radiative transfer – photosynthesis approach. *J Geophys Res* 110:C10014. doi:10.1029/2004JC002784
- Southward AJ, Langmead O, Hardman-Mountford NJ, Aiken J and others (2005) Long-term oceanographic and ecological research in the western English Channel. *Adv Mar Biol* 47:1–105
- Suggett D, Kraay G, Holligan P, Davey M, Aiken J, Geider R (2001) Assessment of photosynthesis in a spring cyanobacterial bloom by use of a fast repetition rate fluorometer. *Limnol Oceanogr* 46:802–810
- Tassan S, Ferrari GM (1995) An alternative approach to absorption measurement of aquatic particles retained on filters. *Limnol Oceanogr* 40:1358–1368
- Teira E, Pazo MJ, Serret P, Fernandez E (2001) Dissolved organic carbon (DOC) production by microbial populations in the Atlantic Ocean. *Limnol Oceanogr* 46:1370–1377
- Tilstone GH, Figueiras FG, Lorenzo LM, Arbones B (2003) Phytoplankton composition, photosynthesis and primary production during different hydrographic conditions at the northwest Iberian upwelling system. *Mar Ecol Prog Ser* 252:89–104
- Tilstone GH, Moore GF, Sorensen K, Doerffer R, Rottgers R, Ruddick KG, Pasterkamp R (2004) REVAMP Protocols; Regional Validation of MERIS chlorophyll products in North Sea coastal waters. Proc Working meeting on MERIS and AATSR Calibration and Geophysical Validation (MAVT 2003), 20–24 Oct 2004. European Space Agency, ESRIN,

- Frascatti, Italy. http://envisat.esa.int/workshops/mavt_2003/MAVT-2003_802_REVAMPprotocols3.pdf
- Tilstone GH, Smyth TJ, Gowen RJ, Martinez-Vicente V, Groom SB (2005) Inherent optical properties of the Irish Sea and their effect on satellite primary production algorithms. *J Plankton Res* 27:1127–1148
- Tilstone GH, Smyth T, Poulton A, Hutson R (2008) Measured and remotely sensed estimates of primary production in the Atlantic Ocean from 1998 to 2005. *Deep-Sea Res II*, doi: 10.1016/j.dsr2.2008.10.034
- Wanninkhof R (1992) Relationship between wind speed and gas exchange over the ocean. *J Geophys Res* 97: 7373–7382
- Weger HG, Herzig R, Falkowski PG, Turpin DH (1989) Respiratory losses in the light in a marine diatom: measurements by short-term mass spectrometry. *Limnol Oceanogr* 34:1153–1161
- Widdicombe CE, Archer SA, Burkill PH, Widdicombe S (2002) Diversity and structure of the microplankton community during a coccolithophore bloom in the stratified northern North Sea. *Deep-Sea Res II* 49:2887–2903
- Williams PJLeB, del Giorgio PA (2005) Respiration in aquatic ecosystems: history and background. In: del Giorgio PA, Williams PJLeB (eds) *Respiration in aquatic ecosystems*. Oxford University Press, New York, p 1–17
- Williams PJLeB, Purdie DA (1991) In vitro and in situ derived rates of gross production, net community production and respiration of oxygen in the oligotrophic subtropical gyre of the North Pacific Ocean. *Deep-Sea Res I* 38:891–910
- Williams PJLeB, Morris PJ, Karl DM (2004) Net community production and metabolic balance at the oligotrophic ocean site, station ALOHA. *Deep-Sea Res I* 51:1563–1578
- Woolf DK, Thorpe SA (1991) Bubbles and the air-sea exchange of gases in near-saturations conditions. *J Mar Res* 49: 435–466
- Yacobi YZ, Perel N, Barkan E, Luz B (2007) Unexpected underestimation of primary productivity by ^{18}O and ^{14}C methods in a lake: implications for slow diffusion of isotope tracers in and out of cells. *Limnol Oceanogr* 52:329–337

*Editorial responsibility: William Li,
Dartmouth, Nova Scotia, Canada*

*Submitted: March 13, 2006; Accepted: September 18, 2008
Proofs received from author(s): December 15, 2008*